

UCLA

UCLA Previously Published Works

Title

Steroid hormone pathways coordinate developmental diapause and olfactory remodeling in *Pristionchus pacificus*.

Permalink

<https://escholarship.org/uc/item/10x478h9>

Journal

Genetics, 218(2)

ISSN

0016-6731

Authors

Carstensen, Heather R
Villalon, Reinard M
Banerjee, Navonil
et al.

Publication Date



2021-06-01

DOI

10.1093/genetics/iyab071

Peer reviewed

Steroid hormone pathways coordinate developmental diapause and olfactory remodeling in *Pristionchus pacificus*

Heather R. Carstensen,¹ Reinard M. Villalon,¹ Navonil Banerjee,² Elissa A. Hallem ,² and Ray L. Hong  ^{1,*}

¹Department of Biology, California State University, Northridge, Northridge, CA 91330-8303, USA and

²Department of Microbiology, Immunology & Molecular Genetics and Molecular Biology Institute, University of California, Los Angeles, Los Angeles, CA 90095, USA

*Corresponding author: Email: ray.hong@csun.edu

Abstract

Developmental and behavioral plasticity allow animals to prioritize alternative genetic programs during fluctuating environments. Behavioral remodeling may be acute in animals that interact with host organisms, since reproductive adults and the developmentally arrested larvae often have different ethological needs for chemical stimuli. To understand the genes that coordinate the development and host-seeking behavior, we used the entomophilic nematode *Pristionchus pacificus* to characterize dauer-constitutive mutants (Daf-c) that inappropriately enter developmental diapause to become dauer larvae. We found two Daf-c loci with dauer-constitutive and cuticle exsheathment phenotypes that can be rescued by the feeding of $\Delta 7$ -dafachronic acid, and that are dependent on the conserved canonical steroid hormone receptor *Ppa*-DAF-12. Specifically at one locus, deletions in the sole hydroxysteroid dehydrogenase (HSD) in *P. pacificus* resulted in Daf-c phenotypes. *Ppa*-*hsd-2* is expressed in the canal-associated neurons (CANs) and excretory cells whose homologous cells in *Caenorhabditis elegans* are not known to be involved in the dauer decision. While in wildtype only dauer larvae are attracted to host odors, *hsd-2* mutant adults show enhanced attraction to the host beetle pheromone, along with ectopic activation of a marker for putative olfactory neurons, *Ppa*-*odr-3*. Surprisingly, this enhanced odor attraction acts independently of the $\Delta 7$ -DA/DAF-12 module, suggesting that *Ppa*-HSD-2 may be responsible for several steroid hormone products involved in coordinating the dauer decision and host-seeking behavior in *P. pacificus*.

Keywords: dauer larva; evolution of development; steroid hormones; molting; olfaction

Introduction

Organisms integrate multiple sensory stimuli from their environment to make key developmental decisions and engage in context-appropriate behaviors. In nematodes, when environmental conditions are unfavorable, a portion of the population can stop feeding and suspend development. Of the several larval stages that can undergo developmental arrest (Zaslaver *et al.* 2011), the dauer larva (DL) in *Caenorhabditis elegans*, as well as the equivalent infective juvenile (IJ) or infective third-larval (iL3) stages in parasitic nematodes, undergo spectacular physiological, morphological, and neuroanatomical changes (Albert and Riddle 1983). At the gene expression level, a number of the dauer entry changes are reversible, while others become permanent life-history traits that mark dauer passage (Lee *et al.* 2017; Vidal *et al.* 2018). Entry into the dauer stage is primarily determined by environmental factors, particularly the depletion of food, elevated temperature, or high levels of ascaroside pheromones in response to overcrowding (Cassada and Russell 1975; Golden and Riddle 1982, 1984a; Jeong *et al.* 2005; Butcher *et al.* 2008).

In *C. elegans*, multiple signaling pathways act in parallel to mediate dauer entry, such as the recognition of pheromones by G-protein-coupled receptors in the chemosensory amphid neurons and signal transduction to the DAF-11/guanylyl cyclase pathway

(Malone and Thomas 1994). In addition, favorable conditions lead to signaling in the DAF-7/TGF- β and DAF-2/insulin-like pathways (Ren *et al.* 1996; Ogg *et al.* 1997; Gems *et al.* 1998). This signaling facilitates the production of $\Delta 4$ - and $\Delta 7$ -dafachronic acid from the cholesterol precursor, which binds the highly conserved nuclear hormone receptor DAF-12 and prevent DAF-12 from repressing genes necessary for development to reproductive adulthood (Dumas *et al.* 2010; Werner *et al.* 2017). Less favorable conditions result in the production of pheromones that reduce signaling in these pathways, subsequently shifting DAF-12 from its inactive ligand-bound form to its active, ligand-free form that specifies dauer development. Despite being a nonfeeding and stress-resistant stage, the DL are actively motile and receptive to external chemosensory and mechanical cues. Like free-living DL, IJs, and iL3s in parasitic nematode species share the ability to survive harsh conditions but remain receptive to semiochemicals from their environment.

In addition to changes in morphology and physiology, dauer development in *C. elegans* also involves rewiring of the sensory nervous system, as well as changes in neuropeptide and chemoreceptor expression (Albert and Riddle 1983; Lee *et al.* 2017; Bhattacharya *et al.* 2019). However, the mechanisms that regulate this remodeling process in other nematodes are largely uncharacterized, thus limiting the scope of generalizable nematode-

Received: April 24, 2020. Accepted: April 26, 2021

© The Author(s) 2021. Published by Oxford University Press on behalf of Genetics Society of America. All rights reserved.

For permissions, please email: journals.permissions@oup.com

wide programs. Comparisons of chemosensory behaviors in reproductive free-living adults vs developmentally arrested DL or iL3s have revealed that responses to some chemosensory cues change dramatically across life stages. For example in *C. elegans*, adults are repelled by carbon dioxide (CO₂) while DL are attracted to CO₂ (Hallem and Sternberg 2008; Hallem et al. 2011). However, most studies of chemosensory behavior in free-living nematodes have been conducted with young adults, while most studies of chemosensory behaviors in parasitic nematodes have been conducted with IJs or iL3s, with very few direct comparisons of chemosensory behaviors between the reproductive and dauer-equivalent stages within the same species (O'Halloran and Burnell 2003; Rasmann et al. 2012; Turlings et al. 2012; Gang and Hallem 2016; Neto et al. 2016; Bryant and Hallem 2018).

The entomophilic nematode *Pristionchus pacificus* is a powerful model system for investigating the genetic network that coordinates dauer entry with development and behavior in host-associated species. In the wild, *P. pacificus* has been found as DL on various species of beetles; upon death of the beetle host, the nematodes exit the dauer state and resume reproductive development to feed on host-associated bacteria (Weller et al. 2010; Mayer et al. 2015, 2017). Thus, the DL of *P. pacificus* is considered to be the host-seeking stage. *P. pacificus* DL have a number of unique adaptations not found in *C. elegans* DL, including an oily coat that promotes aggregation and enhanced survival up to a year (Mayer and Sommer 2011; Penkov et al. 2014). *Pristionchus* adults have distinctive chemosensory preferences for insect pheromones and plant volatiles that differ significantly from those of *Caenorhabditis* species, and also differ across *Pristionchus* species (Hong and Sommer 2006). However, due to the difficulty of obtaining large numbers of DL using the *P. pacificus* reference strain, the chemosensory profiles of *P. pacificus* DL have not yet been examined.

In *P. pacificus*, several dauer formation defective (Daf-d) mutants that fail to form DL under inducing conditions have been isolated by unbiased forward genetics as well as reverse genetics. These studies have identified the genes encoding the nuclear hormone receptor DAF-12 and the forkhead transcription factor DAF-16 as important regulators of dauer formation (Ogawa et al. 2009, 2011). While DAF-12 and DAF-16 functions are conserved between *C. elegans* and *P. pacificus*, mutations in other Daf-d orthologs suggest divergence in the factors that act upstream of these proteins. For example, in *C. elegans*, high-population density induces the secretion of dauer pheromones (Golden and Riddle 1984b; Jeong et al. 2005; Butcher et al. 2008; Schroeder 2015), and mutations in the ascaroside biosynthesis enzyme DAF-22 result in a Daf-d phenotype (Golden and Riddle 1984c). Interestingly, in *P. pacificus*, a recent *daf-22* duplication resulted in subfunctionalization of ascaroside production, but neither mutations in the *Ppa-daf-22.1/daf-22.2* paralogs alone or in combination resulted in defects in dauer formation (Markov et al. 2016). These studies suggest a significant divergence in *P. pacificus* and *C. elegans* dauer regulation upstream of the conserved DAF-12 and DAF-16 modules.

In contrast to the Daf-d mutants, no Dauer formation constitutive (Daf-c) mutants have been genetically characterized in *P. pacificus*, despite forwarding genetic screens and the existence of all of the homologs of the genes responsible for the Daf-c phenotype in *C. elegans*. Putative homologs of the *C. elegans* DAF-11/guanylyl cyclase, DAF-7/TGF- β ligand (7 paralogs), and DAF-2/insulin receptor have been identified in the *P. pacificus* genome (www.wormbase.org), but it remains unknown if any of these homologs are involved in dauer regulation. At the same time,

targeted mutations in the *P. pacificus* heat shock protein *Ppa-DAF-21/HSP90* and *Ppa-DAF-19/RFX* transcription factor affected ciliogenesis but did not result in a Daf phenotype (Sieriebriennikov et al. 2017; Moreno et al. 2018). Because cholesterol is a precursor for the synthesis of steroid hormones needed for both proper ecdysis and dauer formation (Matyash et al. 2004), it remains to be seen if mutations in cholesterol metabolism and steroid signaling are among the yet-undescribed Daf-c mutants in *P. pacificus*.

To identify the unique features and key factors controlling dauer-specific phenotypes in *P. pacificus*, we examined the development and behavior of Daf-c mutants. Previously, a genetic screen in *P. pacificus* yielded four dauer constitutive Daf-c alleles, *dfc* (dauer-formation constitutive), all of which can be rescued by exogenous Δ^7 -dafachronic acid but none has been molecularly cloned (Motola et al. 2006; Ogawa et al. 2009). We, therefore, isolated a new Daf-c allele, *csu60*, and following positional mapping and whole-genome sequencing, found that *csu60* is a null allele of the sole hydroxysteroid dehydrogenase (HSD) in *P. pacificus*, an enzyme responsible for the production of dafachronic acids. For both Daf-c alleles, the DL and adults have olfactory behavior resembling wild-type starvation-induced DL, suggesting that the genes that control dauer entry coordinate host-seeking olfactory behavior.

Materials and methods

Nematode strains

P. pacificus and *C. elegans* strains were maintained at 20°C on NGM plates seeded with OP50 as described previously (Cinkompumin et al. 2014). The following *P. pacificus* strains were used: PS312 (California wild-type, synonymous with RS2333), *Ppa-obi-1(tu404)* ChrI, *Ppa-dfc-1(tu391)* ChrI, and *csu60* ChrII, *Ppa-daf-12(tu389)* ChrX. *csu60* was isolated as an off-target mutant from a CRISPR/Cas9-mediated mutagenesis against a TGF- β ortholog (Contig115-snapTAU.31). Each allele was backcrossed three times to PS312 for the Daf-c phenotype before further characterization. Double mutant with *obi-1(tu404)* was initially selected for the long body phenotype of *obi-1* along with the Daf-c phenotype to create *rlh177(tu391; tu404)* and *rlh192(cs60; tu404)*. Each double mutant with *obi-1(tu404)* was confirmed by sequencing the single nucleotide deletion in *tu404*. The cloning and construction of the *Ppa-odr-3p::rfp(tuEx265)*, *Ppa-odr-7p::rfp(tuEx297)*, and *Ppa-che-1p::rfp(lucEx367)* transgenic lines were described elsewhere (Hong et al. 2019). To examine the expression of these neuronal markers in the *csu60* background, we crossed RFP-expressing transgenic males into *csu60* J4 hermaphrodites, and then established individual transgenic lines from RFP+ F₂ progeny with the Daf-c phenotype.

For F₁ complementation tests, we crossed *dfc-1(tu391); Ppa-daf-6p::rfp* or *csu88; Ppa-che-1p::rfp* males to *Ppa-hsd-2(cs60)* hermaphrodites and looked for the frequency of DL in the RFP+ progeny. We found no DL in 28 RFP+ F₁ progeny for the *tu391* x *csu60* cross, and 14 out of 17 DL in 28 RFP+ F₁ progeny for the *csu88* x *csu60* cross (*P*-values < 0.00001 and 0.2581 respectively when testing for the difference from *csu60* dauer formation, 53 DL/79 total, Fisher's Exact Test). For the epistasis tests, we first crossed *Ppa-daf-12(tu389)* hermaphrodites with *csu60/+* males, then isolated F₂ progeny homozygous for the *csu60* deletion by PCR genotyping and for the single nucleotide substitution of *Ppa-daf-12(tu389)* by Sanger sequencing (Ogawa et al. 2009). The double mutant (*csu60; tu389*) did not produce DL on well-fed or on starved plates, indicating the Daf-d phenotype of *Ppa-daf-12(tu389)* is epistatic to the Daf-c phenotype of *csu60*.

Molecular cloning

To identify the mutations, we first rough mapped the mutation to a chromosomal region using Simple Sequence Length Polymorphic (SSLP) markers on 45 mapping lines generated with the mapping strain RS5278 (Bolivia). Each mapping line was a descendent of a single F₂ DL on nonstarved F₁ plates that exited when we transferred it to a fresh plate of OP50. Nematodes were washed individually from each mapping line in approximate equal pellet sizes prior to pooling and genomic DNA extraction using the MasterPure Kit (Epicentre). We sequenced the whole genome of *csu60* alone well as pooled gDNA from mapping lines (Doitsidou et al. 2010) (~73 million 100 nt reads for each genome and bulk mapping samples; BGISEQ-500 platform with DNA Nanoball technology, BGI America). Rough mapping indicated linkage to Chromosome II, with the additional fine mapping of 47 recombinant lines and the *csu60* genome sequencing revealed a large 95 kb deletion on Chromosome II (1,370,000–1,465,000) that encompassed 10 open reading frames. One of the predicted genes in this interval, PPA10139 (UMM-S10-1.4-mRNA-1 from El Paco whole genome sequence), encodes a 376 amino acid homolog of the *C. elegans* HSD-2.

To make the *Ppa-hsd-2* cDNA rescue transgene, 2063 bp of the *Ppa-hsd-2* promoter was amplified from PS312 genomic DNA using RHL1012 and RHL1013. The full-length *Ppa-hsd-2* cDNA sequence was amplified from PS312 mixed stage cDNA using RHL1014 and RHL1015. The cDNA sequence is identical to UMM-S10-1.4-mRNA-1. The *Ppa-hsd-2* promoter and cDNA were combined with *Ppa-rpl-23* 3' UTR to make pHC12. The mix injected into PS312 adult hermaphrodites contains the following: 2.5 ng/μl pHC12, 4 ng/μl *Ppa-egl-20p::rfp*, 80 ng/μl *csu60* gDNA (all digested with PstI). The transgenic line was then crossed into the *csu60* mutant background using PCR to genotype for the deletion (RHL1006 and RHL1007 will amplify 693 bp if there is a deletion; RHL1043 and RHL1044 will amplify 1008 bp if the same locus is wildtype) and scored as a percentage of dauer or nondauers (J3/J4/adult) containing the rescue transgene. The *csuEx54* transgene transmission rate was approximately 27%.

TurboRFP was introduced downstream of the 2063 bp *Ppa-hsd-2* promoter by Gibson Assembly to make the *Ppa-hsd-2p::rfp* reporter transgene. The injection mix contained PstI digested 5 ng/μl *Ppa-hsd-2p::rfp*, 5 ng/μl *Ppa-egl-20p::rfp*, 80 ng/μl PS312 gDNA.

CRISPR/Cas9 mutagenesis

CRISPR/Cas9 mutagenesis using the roller co-injection marker was used to generate an additional *Ppa-hsd-2* allele *csu88* (Nakayama et al. 2020). Target crRNA, tracrRNA, and Cas9 nuclease were purchased from IDT technologies (San Diego, CA, USA) and hydrated to 100 μM with IDT duplex buffer. An equal volume (0.65 μl) of each of target crRNA (RHL1109) or the co-CRISPR roller crRNA (RHL1123) was mixed with the tracrRNA. The tubes were incubated at 95°C for 5 minutes, followed by room temperature for 5 minutes. Cas9 protein (0.5 μl of 10 μg/μl) was added to each duplex mix and incubated at 37°C for 10 minutes. These two sgRNA products were combined and diluted to a total volume of 40 μl. F₁ and F₂ progeny were screened for the dominant roller phenotype, which were then further examined for mutations in the *Ppa-hsd-2* locus by PCR and sequencing. The roller mutation was then crossed out twice into the PS312 wildtype background before characterization.

Reverse transcription and quantitative real-time PCR

We used two pairs of amplicons with each primer spanning over exon boundaries to determine the relative level of *Ppa-odr-3* transcript expression in *csu60*. cDNA was synthesized using random hexamers (N6) and polyT primers using ~500 ng total RNA from mix staged worms (Thermo Fisher Maxima, M1681). We performed two RNA extractions and three cDNA synthesis to run 12 technical replicates for each of the primer sets. We ran the quantitative real-time PCR (qPCR) reactions using 1–2 μl cDNA in SYBR Green Master Mix (Biorad) totaling 20 μl in a Biorad CFX96 machine using 60°C as the annealing temperature. *Ppa-beta-tubulin* and *Ppa-cdc-42* (RHO GTPase) were used as housekeeping genes and the relative fold change in expression between wildtype and *csu60* was calculated using the delta-delta C_t method (Schuster and Sommer 2012). RT-PCR for *Ppa-hsd-2* and *Ppa-odr-3* transcripts were performed with and without reverse transcriptase as described above.

Phylogeny

The amino acid sequences of potential HSD homologs were first identified by BLASTX searches on WormBase. The phylogeny trees were built using the entire amino acid sequences by first making an alignment and removal of positions with gap using T-COFFEE, followed by Maximum Likelihood phylogeny by PhyML, and finally tree rendering by TreeDyn (www.phylogeny.fr; Dereeper et al., 2008). Midpoint rooting was used and branch support ≥50% is shown.

Temperature response

For each experiment, 10 gravid hermaphrodites were picked onto freshly seeded 6 cm NGM plates and incubated at 15°C, 20°C, or 25°C. Plates were scored for third-stage larvae (active dauer, incarcerated dauer, J3 larvae) after 5 days for *Daf-c* or 3 days for wild-type PS312 (because they starve after 5 days under the same condition). To determine how long the ensheathed DL remain incarcerated, we transferred the immobilized DL at 20°C onto new OP50 NGM plates. After one day at 20°C or 25°C, these cultures were scored for the presence of active DL and incarcerated DL. To determine if J3 or J4 *Daf-c* mutants become incarcerated, we picked the worms onto new OP50 NGM plates at 20°C.

Exogenous Δ7-dafachronic acid

Ten microliter of 75 μM Δ7-dafachronic acid (Gift from Corey Lab and Cayman Chemical) or 100% ethanol vehicle control was mixed into 90 μl OP50 before seeding onto NGM plates. After 2 days, we picked 15–20 *csu60* or *csu88* gravid hermaphrodites onto each plate, which were allowed to lay eggs for 5 hours before being removed for egg synchronization, or if the hermaphrodites lay fewer than 50 eggs they were instead removed after 24 hours. Plates were incubated at 20°C or 25°C for 4–5 days and then scored for DLs and nondauer stages.

Behavioral assays

Pharyngeal pumping rates were observed through a Leica DM6000 upright microscope with a 40x objective, without any anesthetic. J3 larvae, DLs, and incarcerated DLs were mounted onto M9 buffer and 2% agar pads on microscope slides. We counted at least four 15-second intervals per animal, which were then summed to obtain pumps/minute.

Fluorescent red latex beads (Sigma Aldrich, L3280) were used to stage worms and characterize the DLs (Nika et al. 2016).

Overnight OP50 culture was pelleted and resuspended in 1/10 the volume with fresh LB broth. Three microliters of fluorescent beads were added for every 1000 μ l of concentrated OP50, and 100 μ l of this mixture was seeded onto each NGM plate. Plates were used immediately after drying or stored at 4°C for up to a week. Approximately 20–30 worms were picked onto the fluorescent bead/OP50 lawn and scored 40–90 minutes later for uptake of fluorescent beads in the gut. Similarly, 20–30 worms were picked into 1 ml of 1% SDS in M9 and assayed for percentage of moving worms after 10 or 40 minutes. To determine the correlation between bead uptake and SDS resistance, dauer, J2d, and J3 larvae from the same culture were placed separately on fluorescent bead/OP50 lawn for 90 minutes and assayed for percentage of moving worms in 1% SDS.

The population chemotaxis assays for *P. pacificus* were performed on covered 10 cm Petri dishes for ~16 hours at 22°C as previously described (Cinkorpumin *et al.* 2014). However, because *P. pacificus* DL are coated with a long-chain polyunsaturated wax ester (nematol) that makes them highly hydrophobic (Penkov *et al.* 2014), we modified the chemotaxis assay by adopting a chemotaxis medium containing a detergent (10 mM MOPS pH 7; 2.5% Tween 20; 1.5% Bacto-agar) (Nuttley *et al.* 2002). This MOPS/Tween medium promotes both adult and DL dispersal, which when 5% rather than 10% ZTDO was used as an attractant, likely contributed to the slightly higher CI values for PS312 and *obi-1(tu404)* adults than expected compared to previous studies (Cinkorpumin *et al.* 2014). DLs were loaded to the center of the plate by placing and removing immediately a 1 cm² agar chunk from a culturing plate containing either wild-type dauers from starved cultures or *Daf-c* DL from densely populated cultures. We were unable to perform chemotaxis assays on the DL of *obi-1(tu404)* mutants due to its high DL mortality rate, especially in the presence of ZTDO (Cinkorpumin *et al.* 2014). Young adult worms from nearly saturated cultures were washed twice with M9 buffer and collected by centrifuging at 2500 rpm for 2 minutes. Approximately 100 worms were loaded onto each assay plate. Assays with *obi-1(tu404)* DL could not be successfully performed due to their fragility and higher mortality. To anesthetize animals at the odor sources, we placed 1.5 μ l of 1 M sodium azide on both sources and used 100% ethanol as the counter attractant. Multiple assay replicates constituted each experimental trial, and multiple trials were conducted for each condition. All odorants were diluted with ethanol to the following concentrations: 5% (Z)-7-tetradecene-2-one (previous studies used 10% ZTDO, which resulted in more DL paralysis at loading), 1% methyl myristate, 1% (E)-11-tetradecenyl acetate, 1% (Z)-11-hexadecenal, and 10% β -caryophyllene. Interestingly, we found sodium azide to be superfluous when using ZTDO as the attractant due to ZTDO's paralyzing effects on DL. Chemicals were purchased from Fisher Scientific, Sigma-Aldrich, or Bedoukian Research (Danbury, CT, USA).

CO₂ chemotaxis assays

Young adults were washed off plates using M9 buffer and collected in a 65 mm-Syracuse watch glass. Animals were then washed 2X with M9 buffer followed by 1X with sterile water and immediately transferred to the center of 6 cm MOPS/Tween agar plates. Excess water was removed with Whatman paper. DLs were directly transferred to the 6 cm MOPS/Tween agar plates on chunks of agar from starved plates. A CO₂ gradient was generated by delivering specific compositions of gasses through holes in the plate lids as previously described (Carrillo *et al.* 2013). A certified gas mixture containing 21% O₂, balance N₂ (Airgas) air control

was pumped through one hole whereas a certified gas mixture containing 10% CO₂, 21% O₂, balance N₂ (Airgas) was pumped through the other hole. Gasses were pumped through 1/4-inch flexible PVC tubing using a syringe pump (PHD2000, Harvard Apparatus) at a flow rate of 0.5 ml/minutes. Adults and DL were allowed to migrate in the CO₂ gradient for 1 hour and 90 minutes, respectively. Scoring regions were defined as opposite halves of the assay plate 1 cm away from the center line. At the end of the assay, animals that migrated to opposite scoring regions were scored according to the formula:

$$\text{Chemotaxis index (CI)} = \frac{[(\# \text{ animals at CO}_2 \text{ side}) - (\# \text{ animals at air side})]}{(\text{Total } \# \text{ animals at both sides})}$$

As a control for directional bias, two assays were always run simultaneously with CO₂ gradients in opposite directions. Assays were discarded if the difference in the CI between the two plates was ≥ 0.9 or if fewer than 7 animals moved to both scoring regions combined on either assay plate.

Ppa-hsd-2 transgenic rescue of *csu60*

15–20 gravid *csu60* hermaphrodites with or without the *Ppa-hsd-2* transgenic rescue construct were picked onto plates with food, and allowed to lay eggs for 24 hours before removal to obtain a roughly synchronized population of embryos. The plates were incubated at 20°C for 5 days, then scored for DLs and nondauer stages, as well as for the expression of the co-injection marker *Ppa-egl-20p::rfp* as a proxy for the presence of the *Ppa-hsd-2* rescue transgene. Interestingly, we found that this method of synchronizing embryos led to a higher percentage of the population remaining as DL, compared to not synchronizing the embryos used in the temperature sensitivity assay.

Statistical analysis

Statistical tests were analyzed using GraphPad Prism 8 (La Jolla, CA, USA) and Microsoft Excel. We used t-tests or ANOVAs with post-tests for parametric data, and Kruskal-Wallis tests with post-tests for nonparametric data.

Data availability

Strains and plasmids are available upon request. Genome and transcript sequences are available on www.wormbase.org and www.pristionchus.org. The Reagent Table contains additional details on materials and databases. The *csu60* whole genome-sequence is available in figshare at DOI: 10.6084/m9.figshare.14502177. Supplementary material is available in figshare: <https://doi.org/10.25386/genetics.14498556>.

Results

Daf-c mutations act upstream of the conserved DAF-12 NHR

We isolated a constitutive dauer-formation mutant at 20°C, *csu60*. When compared to the only other viable but uncloned *Daf-c* allele, *Ppa-dfc-1(tu391)* from a previous study, we found that both alleles are incompletely penetrant, recessive, and nonallelic for *Daf-c*. In *C. elegans* under reproductive conditions, the binding of the nuclear hormone receptor DAF-12 to steroid hormones, including $\Delta 7$ -dafachronic acids ($\Delta 7$ -DA), restrain L2 larvae from becoming DL, which is a conserved function among diverse nematodes, including *P. pacificus* (Motola *et al.* 2006; Ogawa *et al.* 2009). To determine if the *Daf-c* phenotype of *csu60* or *tu391* is due to a deficiency in DA, we tested a synthetic DA for its ability

to rescue the Daf-c phenotype. Previous work has shown that the constitutive dauer formation phenotype of *dfc-1(tu391)* could be rescued by feeding the worms *Escherichia coli* OP50 containing 7.5 μ M Δ 7-DA (Ogawa et al. 2009). Synthetic Δ 7-DA has been shown to prevent dauer formation in both *P. pacificus* and the ruminant parasite *Strongyloides papillosus* (Ogawa et al. 2009). We found that both the dauer-specific exsheathment defect (see below) as well as the constitutive dauer-formation phenotype of *tu391* and *csu60* were rescued by the availability of Δ 7-DA in the food (Figure 1, A and B). These results suggest that both mutants cannot produce sufficient dauer-suppressing Δ 7-DA.

To further confirm this genetic pathway for dauer regulation by epistasis analysis, we constructed *csu60*; *daf-12(tu389)* double mutants and found that they resembled the Daf-d phenotype of *daf-12(tu389)* (Ogawa et al. 2009) (Supplementary Table S1), consistent with the expected position of *csu60* acting upstream of the nuclear hormone receptor. Similarly, the *dfc-1(tu391)*; *daf-12(tu389)* double mutants completely masked the Daf-c phenotypes of *tu391*, placing *tu391* also upstream of *daf-12* for the regulation of dauer formation. Hence, *daf-12* is epistatic to both *csu60* as well as *tu391*. Curiously, a small percentage (3.7%) of the *csu60*; *daf-12(tu389)* double mutants exhibited an ecdysis defect in the molts between the late larval stages (J3-J4; J4-adult), rather than J2-DL, which is a synergistic phenotype not found in either mutant alone (Supplementary Table S1). Both Daf-c mutations thus act through the Δ 7-DA/DAF-12 module critical for DL formation.

Molecular cloning of the first *P. pacificus* Daf-c locus

Using the latest genome assembly of *P. pacificus*, we performed whole-genome sequencing of *csu60* and identified a \sim 95 kb deletion on Chromosome II that affected 10 predicted protein-coding genes, 6 of which have transcript support (Werner et al. 2018). Among these candidates, the predicted protein sequence of PPA10139 is orthologous to the 3 Δ -hydroxysteroid dehydrogenase/ Δ 5- Δ 4 isomerases (3 Δ -HSDs) that are key steroidogenic enzymes in vertebrates (GO:0003854). PPA10139 shares 89% similarity with *C. elegans* HSD-2, which encodes one of three HSDs in *C. elegans* involved in the biosynthesis of dafachronic acids (Patel et al. 2008; Dumas et al. 2010). Consistent with its potential role in repressing dauer formation, PPA10139 transcript levels are lower

in DL relative to the reproductive developmental stages (Baskaran et al. 2015).

To determine if the Daf-c phenotype of *csu60* is due to a deficit in *Ppa-hsd-2*, we made a construct containing a \sim 2 kb promoter of PPA10139 driving its full-length cDNA to rescue the *csu60* deletion by transgene complementation. Worms containing the transgenic *Ppa-hsd-2p::cDNA* extrachromosomal array showed dramatically lower constitutive dauer formation, and lower rates of the dauer-specific exsheathment phenotype, than *csu60* siblings without the transgene (Figure 1C).

We then investigated the possible evolutionary history of *hsd* genes in nematodes. We found only one putative ortholog of HSD-2 in each of the completed genomes of the human parasites *B. malayi* and *Onchocerca volvulus*, whereas the *C. elegans* genome contains three paralogs, suggesting that a single HSD is likely the ancestral state (Figure 2A). Each *hsd* gene in *C. elegans* differs by the number of transmembrane domains: *hsd-1* encodes for two predicted transmembrane domains, *hsd-2* encodes for one transmembrane domain, while *hsd-3* does not encode for any predicted transmembrane domain (as predicted by SMART utilizing TMHMM). Although the overall protein sequence of PPA10139 shares the highest similarity to *C. elegans* HSD-2, the two transmembrane domains predicted for *Ppa-HSD-2* argues for more functional similarity to *C. elegans* HSD-1. Furthermore, while the *C. elegans* *hsd-1* is located on Chromosome I, the *C. elegans* *hsd-2* and *hsd-3* appear to be recent gene duplications on Chromosome X, suggesting that the appearance of the *P. pacificus* *hsd-2* locus on Chromosome II (syntenic with *C. elegans* Chromosome II) preceded the divergence of these two species (Rödelsperger et al. 2017).

To determine if the loss of *Ppa-hsd-2* is sufficient to cause the Daf-c phenotype, we generated additional alleles by targeted mutagenesis using CRISPR/Cas9 (Witte et al. 2015; Han et al. 2020; Nakayama et al. 2020). We identified another allele, *csu88*, which did not have a mutation near the crRNA site (Figure 2B), but did exhibit the Daf-c and dauer exsheathment defect characteristic of *csu60* (Supplementary Table S1). Using PCR, we inferred a \sim 67 kb deletion in *csu88* that extended downstream from the *Ppa-hsd-2* second intron and confirmed the absence of *Ppa-hsd-2* transcripts by RT-PCR (Supplementary Figure S1). Complementation test shows *csu88* could not complement *csu60*, and like *csu60*, the Daf-c phenotype of *csu88* was also rescued by exogenous Δ 7-DA.

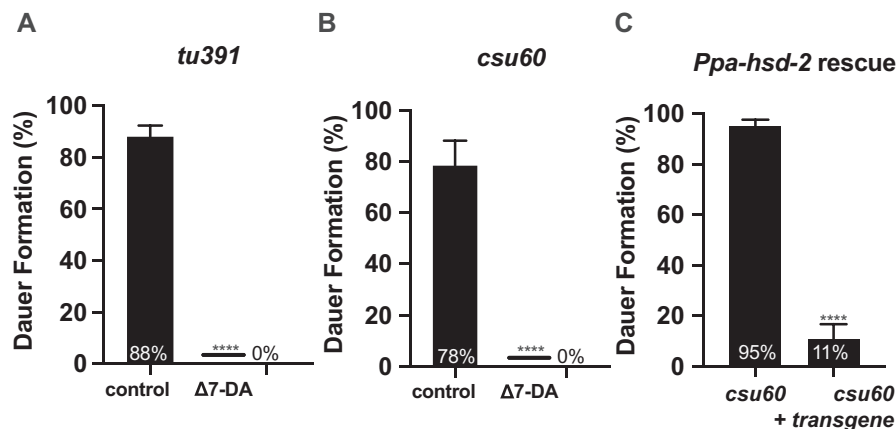


Figure 1 Hormonal and transgenic rescue of Daf-c phenotype. (A, B) The constitutive dauer phenotype in both Daf-c mutant alleles is completely rescued by exogenous Δ 7-dafachronic acid but not by the ethanol control. (t-test between mock and DA treated. **** P < 0.0001. Sample size: *tu391* control = 435; *tu391* treated = 426; *csu60* control = 210; *csu60* treated = 284). (C) A transgene carrying the *Ppa-hsd-2* promoter driving its own cDNA strongly rescues the constitutive dauer and exsheathment defects in *csu60* (t-test between transgenic and nontransgenic populations. **** P < 0.0001; Sample size: *csu60* = 2246; *csu60* with the rescue transgene = 2388). Dauer formation is the percentage of DL in all third-stage larvae or older.

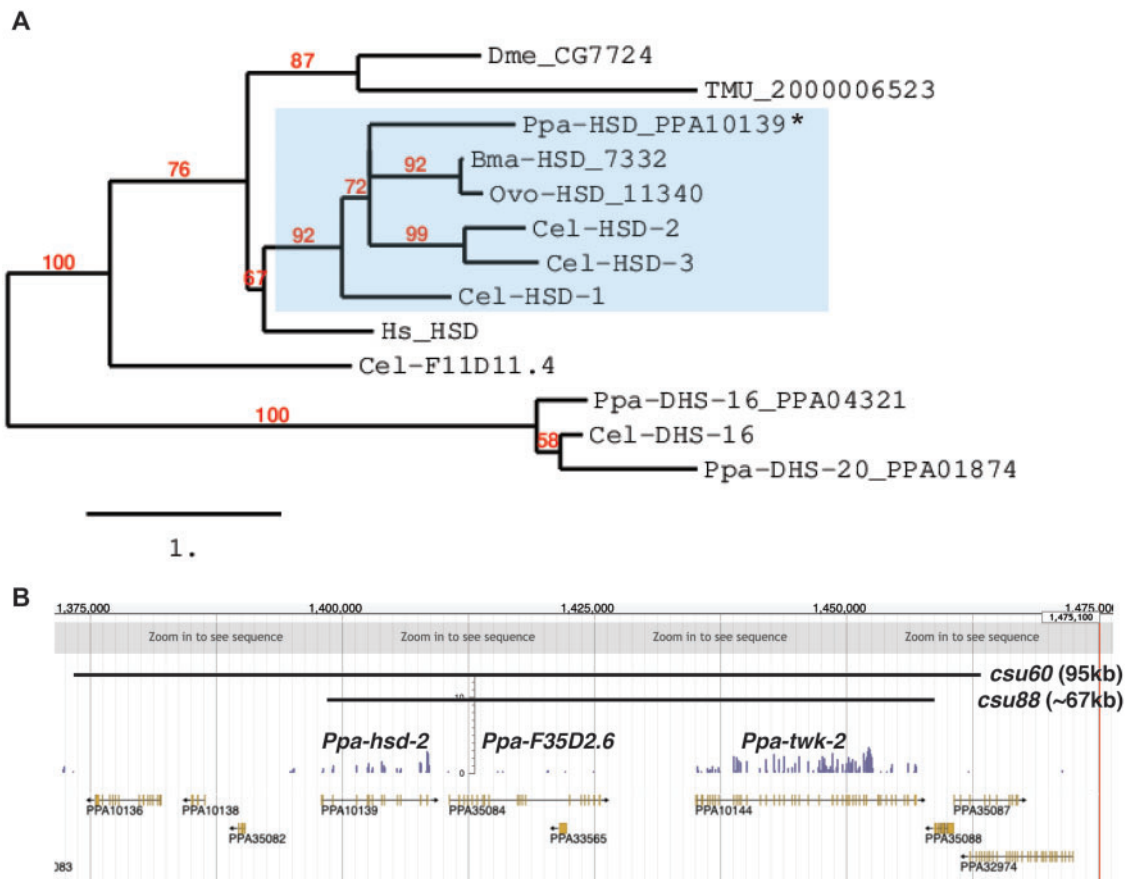


Figure 2 *Ppa-hsd-2* phylogeny and the *Daf-c* locus. (A) Orthology assignment for **Ppa-HSD-2* (PPA10139). Maximum likelihood phylogeny trees were generated by PhyML (phylogeny.fr). Midpoint rooting was used and only branch support $\geq 50\%$ is shown. Protein sequences for *P. pacificus* are “Ppa-” (orthology same as Wormbase.org) and for *C. elegans* “Cel-.” Sequences from additional species are *Drosophila melanogaster* (Dme), *O. volvulus* (Ovo), *B. malayi* (Bma), *Trichuris muris* (Tme), and *Homo sapiens* (Hs). Dehydrogenases DHS-16 from *C. elegans* along with DHS-16 and DHS-20 from *P. pacificus* are closest to the HSDs and are used as an outgroup. (B) JBrowse snapshot of the *Daf-c* locus on Chr. II shows *csu60* and *csu88* share a deletion region that encompass *Ppa-hsd-2* (PPA10139), *Ppa-F35D2.6* (PPA35084), and *Ppa-twk-2* (PPA10144) that have transcript support (Rödelsperger et al. 2017).

Thus, a second allele at the *Ppa-hsd-2* locus phenocopies *csu60*, and both transgenic complementation with *Ppa-hsd-2* cDNA and $\Delta 7$ -DA are sufficient to rescue the *csu60* *Daf-c* phenotype.

***Ppa-hsd-2* is expressed in the CAN neurons and excretory-secretory system**

In vivo measurements in *C. elegans* indicated that peak $\Delta 7$ -DA concentration occurs in the L2 prior to the commitment to dauer entry, and that *Daf-c* mutants have DA levels less than 15% of that in wild-type L2s (Li et al. 2013). To determine the stage-specific expression patterns of *Ppa-hsd-2*, we examined two independent transgenic reporter strains containing the ~2-kb promoter of *Ppa-hsd-2*. We found that the cell type that expressed the transgene most robustly at every developmental stage is the canal-associated neurons (CANs), whose cell body are near the midbody with processes that run along the excretory canal laterally along most of the body (Figure 3; Supplementary Table S2). In *C. elegans*, CAN neurons are required for survival but little is known about their function (White et al. 1986). Whether they function as neurons is also unclear due to their lack of synaptic connections (White et al. 1986). In contrast, in *P. pacificus*, the ablation of the CAN neurons resulted in an enhanced response to dauer pheromone (Mayer et al. 2015). All developmental stages also show *Ppa-hsd-2p::rfp* expression in a few intestinal cells as well as the excretory gland cell, though expression in the excretory canal was detectable only in the dauer stage (Figure 3, A and E–G). We

speculate that the CAN neurons *P. pacificus* could innervate the excretory cells, given that the anterior CAN neuron processes reach the nerve ring (Figure 3A). Thus, the *Ppa-hsd-2* expression pattern is most prominent in the excretory-secretory system and in the CAN neurons, which are known to inhibit dauer formation in *P. pacificus*.

***Daf-c* mutations enhance adult chemotaxis response**

Since there have been no studies on the chemosensory behavior of *P. pacificus* DL, we sought to take advantage of the high proportion of active *Daf-c* DL using a modified assay to look for potential behavioral changes between *P. pacificus* young adults and DL. First, to determine if *Daf-c* DL behave similarly to wild-type DL, we tested DL of wildtype, *tu391*, and *csu60* with a panel of odors that are known attractants for *P. pacificus* adults. We focused on the Oriental beetle pheromone (Z)-7-tetradecene-2-one (ZTDO) and the fly aggregation pheromone methyl myristate and found that the DL of wildtype and *csu60*, and to a lesser extent *tu391*, exhibited strong attraction to both of these insect host pheromones (Figure 4A). Given this wild-type chemosensory response by the *Daf-c* DL, we expanded the survey of DL chemosensation to the insect pheromones E-11-tetradecenyl acetate (ETDA) and hexadecenal, as well as the plant defense volatile β -caryophellene, which are all known attractants for *P. pacificus* adults, but found that neither *Daf-c* nor wild-type DL responded to these

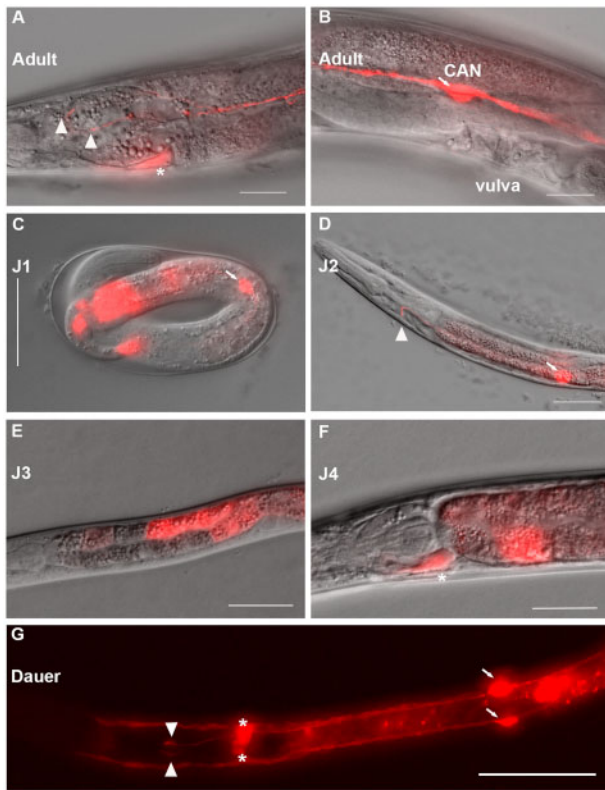


Figure 3 *Ppa-hsd-2* is expressed in multiple cell types. Representative DIC and fluorescent overlay images of (A, B) an adult with *Ppa-hsd-2p::rfp* expression in the excretory gland cells (*) and in the pair of CAN neurons (arrow). The anterior CAN processes are visible near the pharyngeal isthmus (triangles) (C) The earliest *Ppa-hsd-2* expression is in the CAN neurons of J1 larvae prior to hatching. (D) CAN neuron expression in a J2 larva. (E) Intestine expression in a J3 larva. (F) Excretory gland cell and intestine expression in a J4 larva. (G) Ventral max projection of a DL, which is the only developmental stage that shows *Ppa-hsd-2* expression in the excretory canal. Images were taken at 250–525 ms exposure. Sample sizes are shown in Supplementary Table S2. Scale bar: 25 μ m.

odorants (Supplementary Figure S2A) (Herrmann et al. 2007; Hong et al. 2008). We also examined the responses of Daf-c DL to a panel of *C. elegans* attractants: 2,3-butanedione (diacetyl), 2,3-pentanedione, and isoamyl alcohol (Bargmann et al. 1993). We found that like *P. pacificus* adults, the DL also did not respond to these low molecular weight chemicals (Supplementary Figure S2B). Thus, DL exhibited near wild-type responses to two known insect-associated odors but have a narrower overall odor response profile compared to adults.

To better define the genetic pathways that are responsible for the chemosensory differences between the host seeking DL and reproductive adults, we focused on the responses of the *Ppa-hsd-2* mutants to a host pheromone, ZTDO (Cinkompumin et al. 2014). We observed that wild-type PS312 showed the strongest difference between the DL and adults, with an almost threefold stronger attraction in DL than in adults (Figure 4B). We also observed significantly stronger attraction by the adults of both *Ppa-hsd-2* alleles compared to wildtype, such that there is no difference between the responses of DL and adult stages of *csu60* and *csu88* (Figure 4B). Because the passage through the dauer stage may introduce lasting post-dauer changes that alter odorant receptor expression and hence modulate behavior (Sims et al. 2016; Vidal et al. 2018; Pradhan et al. 2019), we also examined the ZTDO

response of wild-type post-dauer adults. We found that dauer passage alone did not result in enhanced ZTDO response in adults (Figure 4C). Thus, genes that inhibit dauer development also repress the ZTDO attraction in adults.

To determine how the *Ppa-hsd-2* mutants interact with chemosensory mutants mediating the ZTDO response, we examined the chemotaxis behavior of the *Ppa-hsd-2(csu60)* mutants in the loss-of-function *obi-1(tu404)* background that is defective for its cGMP-dependent responses to ZTDO (Cinkornpumin et al. 2014). We found that the loss of *obi-1* significantly reduced the ZTDO response in *csu60* adults as well as DL, though DL still showed more attraction to ZTDO than adults (Figure 4B). Interestingly, while *Ppa-daf-12* is epistatic to *csu60* in dauer formation, *csu60; daf-12(tu389)* double mutant adults still exhibited the *csu60* enhanced attraction to ZTDO (Figure 4D). Furthermore, whereas exogenous $\Delta 7$ -DA rescued the Daf-c phenotype but did not rescue the enhanced host pheromone attraction in adults, the *Ppa-hsd-2p::cDNA* transgene rescued the *csu60* enhanced chemotaxis phenotype (Figure 4E). Thus, the regulation of chemotaxis responses can be uncoupled from dauer formation. Taken together, our results suggest that the enhanced pheromone attraction of adult *Ppa-hsd-2(csu60)* depends on *obi-1* but not the $\Delta 7$ -DA/DAF-12 module.

CO₂ is repulsive to both adults and DL

Since host odor attraction in IJs of entomopathogenic nematodes (EPN) is enhanced by CO₂, we next tested the chemotaxis response of *P. pacificus* DL to CO₂ (Hallem et al. 2011; Dillman et al. 2012). In *C. elegans*, well-fed adults are repelled by CO₂, while DLs are attracted to the same concentration (Hallem and Sternberg 2008; Hallem et al. 2011). In *P. pacificus* well-fed adults, CO₂ also elicits a strong avoidance response which, as in *C. elegans*, is mediated by a pair of internal gas sensing neurons known as the BAG neurons (Hallem and Sternberg 2008). To determine if CO₂ response valence also differs between *P. pacificus* DL and adults, we examined the response to CO₂ in Daf-c DL and adults using the modified chemotaxis assay. We found that wild-type *P. pacificus* DL exhibited a slightly stronger avoidance response than adults, while both Daf-c DL and adults showed equally robust repulsion by CO₂ (Figure 5). Thus, unlike the enhanced response to the beetle host pheromone, wild-type *P. pacificus* DL did not exhibit a valence change to CO₂. Interestingly, iL3s of the mammalian parasites *S. stercoralis*, *S. ratti*, *Ancylostoma ceylanicum*, and *Nippostrongylus brasiliensis* are also repelled by CO₂ (Castelletto et al. 2014; Ruiz et al. 2017). It is currently unclear how the CO₂ avoidance response of *P. pacificus* DL, but not *C. elegans* DL, factors into the different life strategies of these two species in their respective ecologies.

The *Ppa-hsd-2* locus affects amphid neuron identity

Given the finding that *P. pacificus* HSD-2 is upstream of the putative branching point for dauer formation and olfaction, we sought to investigate possible neuronal type changes associated with the enhanced attraction to ZTDO in *csu60* and *csu88* adults. Using their connectivity profiles and axon trajectories, recent comparisons of the neuroanatomy between *C. elegans* and *P. pacificus* identified homologs of the two pairs of amphid olfactory neurons responsible for odor attraction, AWA, and AWC (Hong et al. 2019). The *P. pacificus* AWC homolog, AM7, expresses *Ppa-odr-7p::rfp* (rather than the G-protein-coding *odr-3* in *C. elegans*), whereas the AWA homolog, AM3, expresses *Ppa-odr-3p::rfp* (rather than the nuclear hormone receptor-coding *odr-7* in *C. elegans*). We found

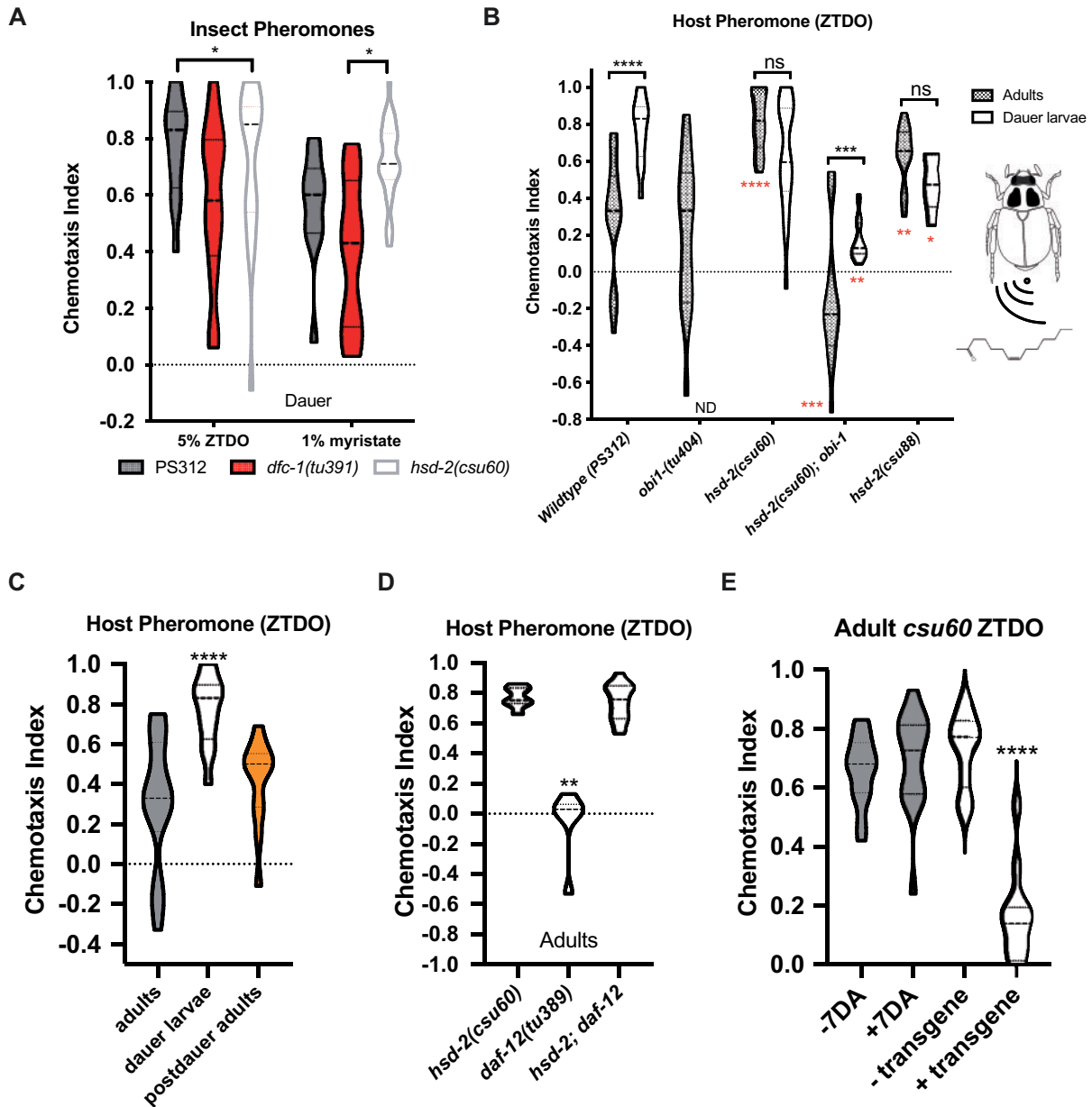


Figure 4 Olfactory responses of *P. pacificus* DLs. (A) DLs of wild-type and *Daf-c* mutants show robust attraction to 5% Oriental beetle pheromone z-(7)-tetradecen-2-one (ZTDO) and 1% house fly aggregation pheromone methyl myristate. Two-way ANOVA with Dunnett's multiple comparisons test to wildtype. Sample sizes: *dfc-1* ZTDO = 764, *csu60* ZTDO = 324, PS312 ZTDO = 272, *dfc-1* myristate = 743, *csu60* myristate = 1502, PS312 myristate = 136. For each category, 10–33 assays were performed over at least 2 trials. (B) *Ppa-hsd-2* alleles have enhanced adult attraction to the host beetle pheromone ZTDO that is dependent on *obi-1*. Red asterisks indicate differences to PS312 by genotype using One-way ANOVA with Dunnett's (adult) or Kruskal-Wallis test (DL); Black asterisks indicate differences between adults and dauer by multiple unpaired t-test using Sidak's method. Sample sizes: PS312 adults = 272, PS312 DL = 315, *obi-1* adults = 219, *csu60* adults = 397, *csu60* DL = 544, *csu60*; *obi-1* adults = 227, *csu60*; *obi-1* DL = 1352, *csu88* adults = 541, *csu88* DL = 257. PS312 and *csu60* DL are the same data as in 4A, with extra replicates for *csu60* DL. For each category, 13–33 assays were performed over at least 2 trials. (C) PS312 Post-dauer adults show a similar response to ZTDO as the never-dauer adults. Significance is shown relative to the adults. One-way ANOVA with Dunnett's *post-hoc* test. Sample sizes: adults = 345, DL = 315, post-DL adults = 255. Adults and DL are same data as 4B, with extra replicates for adults. 12–18 assays were performed over at least 2 trials. (D) The steroid hormone receptor encoded by *Ppa-daf-12* is not required for the enhanced attraction to ZTDO in adult *csu60*. One-way ANOVA with Kruskal-Wallis test. Sample sizes: *csu60* = 596, *daf-12* = 304, *csu60*; *daf-12* = 1830. 7–16 trials were performed over at least 2 trials. (E) Adults from *hsd-2(csu60)* cultures grown on exogenous Δ^7 -dafachronic acid (7DA) exhibited the same enhanced ZTDO attraction as ethanol-treated adults, but the *Ppa-hsd-2p::cDNA* transgene rescued the enhanced ZTDO odor attraction of *csu60* adults to unresponsive ($P < 0.0001$, two-way ANOVA). Sample sizes: -7DA = 729; +7DA = 1418; no transgene = 727; transgene = 358. For each category, 9–16 assay replicates were performed over three trials. Violin plots show median with quartiles.

that while *Ppa-odr-7p::rfp* expression is unaltered in *Ppa-hsd-2(csu60)* mutants (Supplementary Figure S3, A and B), *Ppa-odr-3p::rfp* expression is dramatically altered in *csu60* in all post-hatching stages (Figure 6). Specifically, in addition to the robust *Ppa-odr-3p::rfp* expression in AM3(AWA) and the weaker

expression in AM4(ASK), 68% of *csu60* J4 larvae and adults also showed unexpected expression in a third pair of amphid neurons posterior to the AM3(AWA) (Figure 6; Supplementary Table S3). *Ppa-hsd-2(csu88)* adults also showed ectopic *Ppa-odr-3p::rfp* expression in this extra pair of amphid neurons (Figure 6;

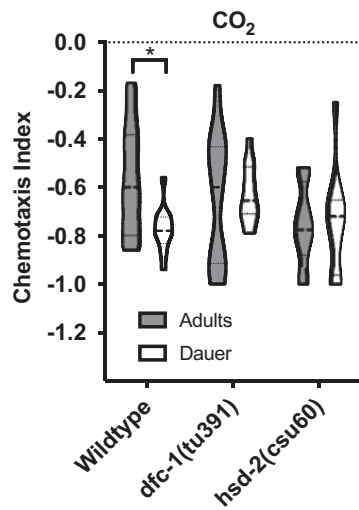


Figure 5 *P. pacificus* is repulsed by CO₂. The response to CO₂ differs slightly between wild-type adults and dauers, but does not differ between adults and DLs in the *Daf-c* mutants. Significance is shown between adults and DL; Two-way ANOVA with Sidak's method. Sample sizes: PS312 adults = 363, PS312 DL = 243, *dfc-1* adults = 439, *dfc-1* DL = 334, *csu60* adults = 299, *csu60* DL = 155. For each category, 12 assays were performed over three trials. Violin plots show median with quartiles. **P* < 0.05; ***P* < 0.01; *****P* < 0.001, ******P* < 0.0001.

Supplementary Table S3). The level of *Ppa-odr-3p::rfp* expression was also stronger in *csu60* and *csu88* compared to wildtype, although it is not clear if the expression represents a duplication of the AM3(AWA) or the AM4(ASK) cell fate.

We then sought to determine if exogenous $\Delta 7$ -DA can suppress the ectopic *Ppa-odr-3p::rfp* expression but found that while the same level was sufficient to suppress the *csu60* *Daf-c* phenotype, $\Delta 7$ -DA could not suppress the ectopic *Ppa-odr-3p::rfp* expression (Supplementary Table S3). Finally, to confirm that the increased *Ppa-odr-3* promoter activity and ectopic cellular expression correspond to increased overall *Ppa-odr-3* mRNA transcripts in *csu60*, we performed qPCR on mix-stage cultures and found that *Ppa-odr-3* transcripts are indeed ~ 10 -fold higher in *csu60* than in wildtype (Supplementary Figure S4).

These findings suggest that HSD activity suppresses a default-on *Ppa-odr-3*-expressing cell fate prior to hatching in the J1 larvae or during embryogenesis. Because the duplicated *Ppa-odr-3p::rfp* pair was not found in wild-type DL, which show attraction to ZTDO, the difference in the *odr-3p::rfp* expression pattern alone cannot not fully explain the stronger ZTDO attraction in DL compared to adults in wildtype, but is consistent with the possibility that the transformed wild-type amphid neuron may be involved in restricting dauer entry.

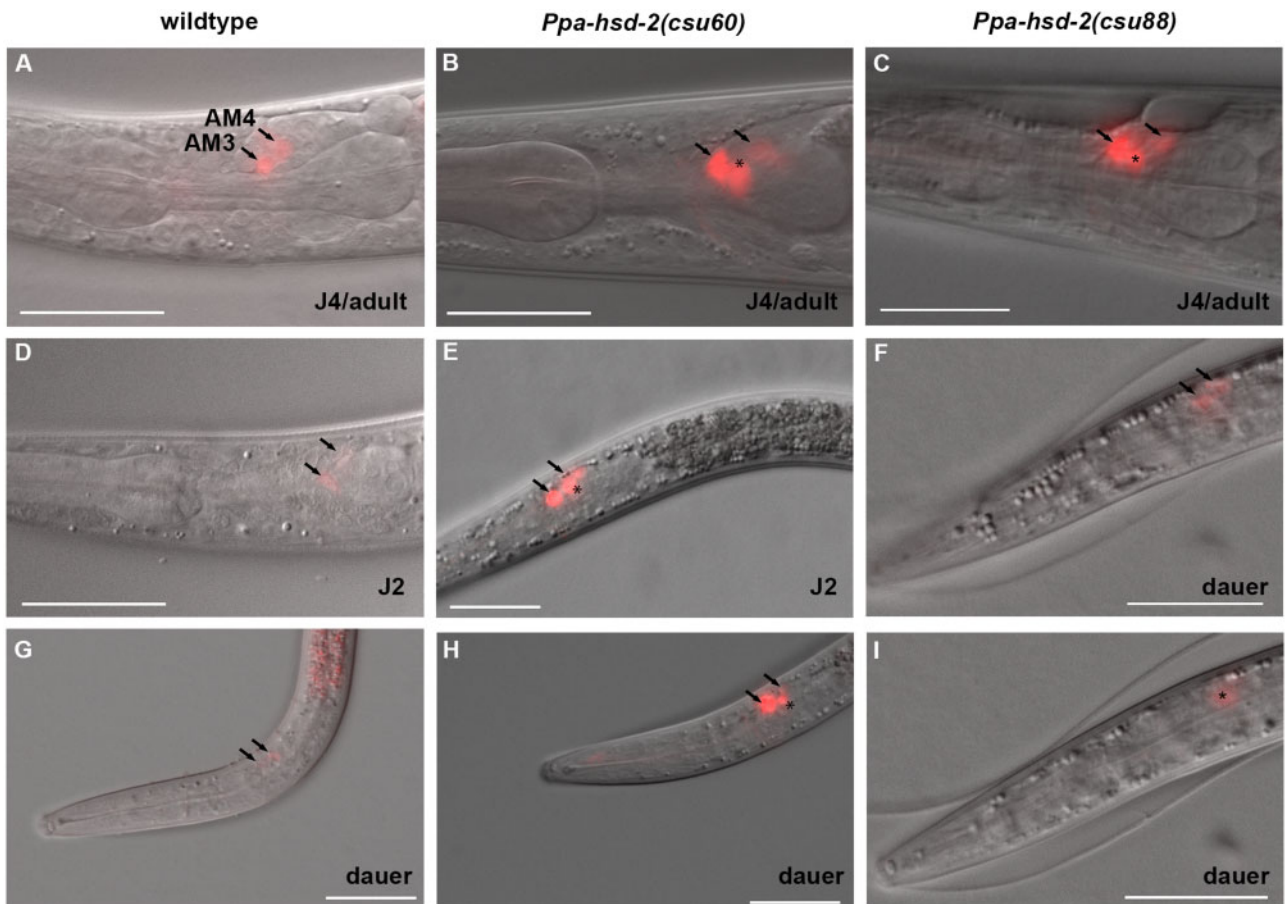


Figure 6 Ectopic *Ppa-odr-3p::rfp* expression in amphid neurons of *Ppa-hsd-2* mutants. (A–C) Representative DIC and fluorescent overlay images of J4 and adults. In wildtype, *Ppa-odr-3p::rfp* expression is found in AM3(AWA) and AM4(ASK) amphid neurons (arrows). In *csu60* and *csu88* mutants, reporter expression in AM3 and AM4 is stronger than wildtype and is found in an additional pair of amphid neurons posterior to the AM3(*). (D–E) *Ppa-odr-3p::rfp* expression in wildtype J2 and ectopic expression in *csu60* J2. (F, I) Ectopic *Ppa-odr-3p::rfp* expression in a *csu88* DL at different focal planes. (G, H) *Ppa-odr-3p::rfp* expression in wildtype DL and ectopic expression in *csu60* DL. Sample sizes are shown in Supplementary Table S3. Anterior is left and dorsal is up. Scale bar: 25 μ m.

Pristionchus pacificus *Daf-c* mutants have a dauer exsheathment phenotype

Akin to the infective L3 stage of parasitic nematodes, we found ~63% of wild-type *P. pacificus* DL under laboratory condition are ensheathed ($n = 122$), in which the sheath is thought to be the apolysed but unecdysed J2 cuticle snugly covering the dauer cuticle. *C. elegans* DL, in contrast, are only very transiently ensheathed (Cassada and Russell 1975). Strikingly, while the ensheathed wild-type DL are motile, both *Daf-c* alleles exhibited an unusual cuticle defect in which active larvae are trapped and immobilized inside an old cuticle (Figure 7, A–C). Aside from the loosened cuticle, the “incarcerated” larvae in *tu391* and *csu60* are indistinguishable from DL produced by the wild-type reference strain PS312 under starvation conditions; they are characterized by radial shrinkage of the body, a darkened intestine, and a buccal cap covering the mouth. In EPN from the genera *Steinernema* and *Heterorhabditis*, ensheathment appears to confer increased ability to resist desiccation, while exsheathment leads to increased motility and is the first step of the host infection process (Campbell and Gaugler 1991; Menti et al. 1997). Our results reveal that in *P. pacificus*, ensheathment is unique to the DL and genetically regulated with dauer entry.

To determine if the incarcerated worms are exclusively in the dauer stage, which does not feed, we measured their pharyngeal pumping frequency (Cassada and Russell 1975). We found that the incarcerated *tu391* and *csu60* larvae display pumping rates significantly lower than the J3 and J4 stages of wild-type and mutant animals, but indistinguishable from their respective non-incarcerated (active) DL siblings as well as wild-type *P. pacificus* and *C. elegans* DL (Figure 7D). We also isolated *tu391* and *csu60* J3 and J4 larvae onto fresh OP50 to determine if they would develop into incarcerated larvae but did not observe incarcerated worms ($n_{J3, tu391} = 60$; $n_{J4, tu391} = 50$; $n_{J3, csu60} = 95$; $n_{J4, csu60} = 100$), suggesting that the molting defect in *tu391* and *csu60* is an exsheathment defect exclusive to the formation of the dauer cuticle. To determine if the incarcerated DL is a permanent or transient phenotype, we picked incarcerated *tu391* and *csu60* DL onto fresh OP50 plates. We found incarcerated *tu391* and *csu60* DL became free and active within 24 hours ($n_{tu391} = 213$; $n_{csu60} = 124$). Taken altogether, the incarcerated worm is a transient dauer-specific phenotype.

Because temperature modulates the dauer decision (Swanson and Riddle 1981; Golden and Riddle 1984b), we wondered if the constitutive dauer formation and the dauer-specific exsheathment defects are temperature-dependent. We found that for

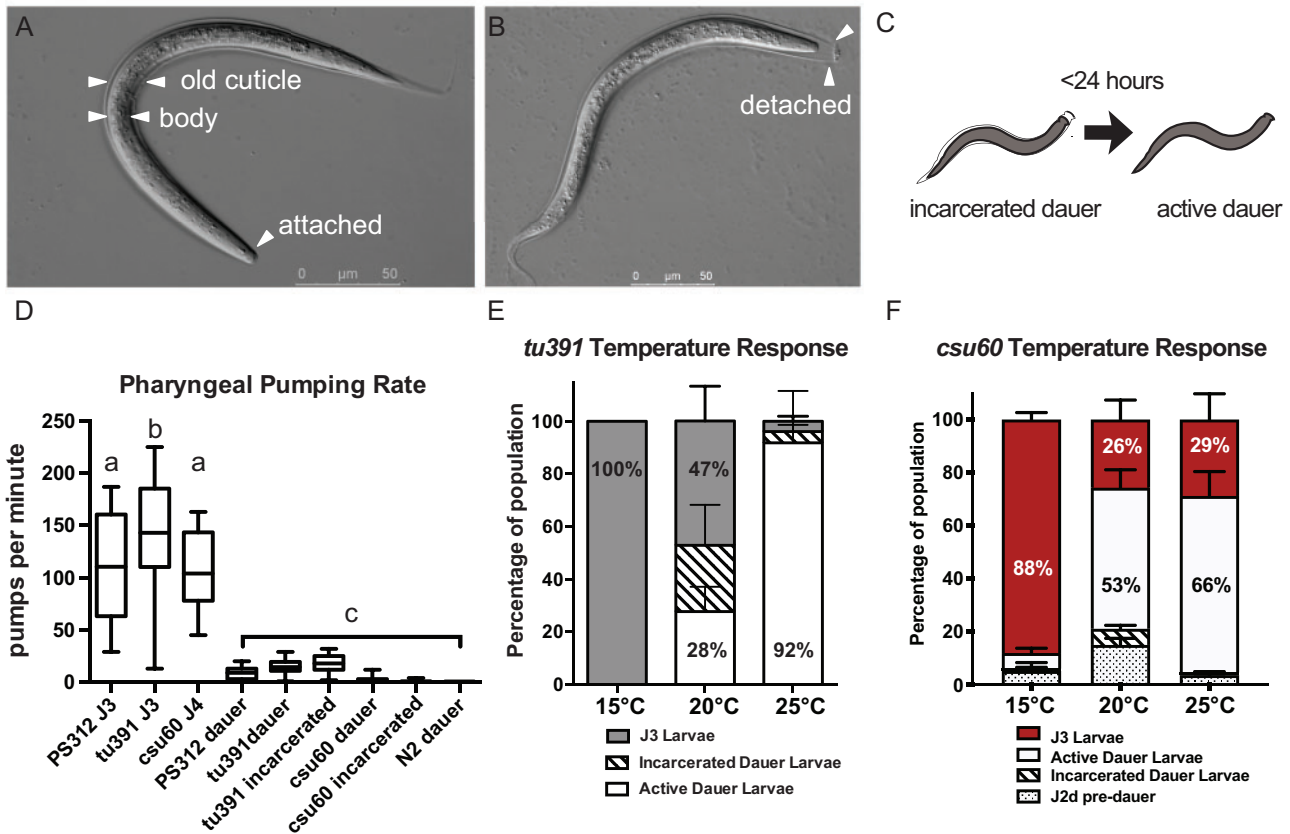


Figure 7 Incarcerated larvae are temperature-dependent constitutive DLs. Ten young adult hermaphrodites on food were transferred to different temperatures for 5 days, and their progeny were then scored for dauer-equivalent J3 stages. (A) Ensheathed wild-type PS312 DLs. The effete J2 cuticle surrounding the body is visible. PS312 DL does not show the incarcerated phenotype. (B) In an incarcerated *tu391* DL, the J2 cuticle is not attached at the head in nearly half of *tu391* constitutive DLs. (C) The illustration depicts that the incarceration is transient. (D) Incarcerated DLs ($n_{tu391} = 22$; $n_{csu60} = 30$) exhibit pharyngeal pumping rates similar to active mutant dauer ($n_{tu391} = 22$; $n_{csu60} = 13$) and wild-type *P. pacificus* and *C. elegans* dauer ($n_{Ppa} = 24$; $n_{Cel} = 18$), which are significantly different from that of the J3 and J4 larval stages (PS312 J3 $n = 32$; *tu391* J3 $n = 40$; *csu60* J4 $n = 13$) (letters denote significant differences at $P < 0.001$, one-way ANOVA, Tukey’s multiple comparisons post-test). (E) The proportions of *tu391* J3 larvae, active DLs, and DLs differ at 15°C ($n = 577$), 20°C ($n = 2091$), and 25°C ($n = 1622$). Wild-type PS312 is 100% J3 at all temperatures. (F) The proportion of *csu60* J3 to DLs differ between 15°C ($n = 1090$) and the higher temperatures 20°C ($n = 2846$) and 25°C ($n = 2516$). Incarcerated DLs with exsheathment defect are most abundant at 20°C. Additional details are found in Supplementary Table S1 and Figure S5.

tu391, lower temperature (15°C) completely suppressed the *Daf-c* phenotype, while higher temperature (25°C) promoted the highest proportion of DL (92% of third-stage larvae) but dramatically suppressed the dauer incarceration defect (Figure 7E, Supplementary Table S1). Similarly, for *csu60*, free DL formation was highest at 25°C (66%) compared to 15°C (6%), although the increase at 25°C compared to 20°C (53%) was noticeably less than the effect observed for *tu391*. Like *tu391*, the highest proportion of *csu60* incarcerated DL occurred at 20°C (6%) (Figure 7F, Supplementary Table S1, Figure S5). Thus, increasing the temperature resulted in higher DL formation in both alleles, while the incarcerated defect was most prevalent at 20°C. It is unclear if higher temperature suppresses the initiation of the exsheathment defect or shortens the duration of the incarceration. These findings indicate that the *Daf-c* mutants in *C. elegans* and *P. pacificus* both promote dauer formation at higher temperatures, but DL formation in *csu60* is less sensitive to temperature than in *tu391*, suggesting the genes responsible for these loci occupy different positions in the *P. pacificus* dauer regulation pathway.

Daf-c mutants reveal a dauer-committed J2 stage

In addition to the cuticle exsheathment phenotype, we also observed the occurrence of partial DLs with *csu60*; in contrast, partial DLs were not observed with wild-type or *tu391* animals. These incomplete dauers exhibited a dark intestine and lethargy typical of DL, but lacked the radial constriction and buccal cap that also define DL (Figure 8, A and B). After hatching, *C. elegans* L1 larvae can either enter the reproductive development pathway and become L2 larvae, or they can become pre-dauer L2s larvae when treated with exogenous dauer-inducing pheromones. The pre-dauer L2d larvae can either return to reproductive development or enter the dauer diapause pathway, depending on the concentration of dauer-inducing pheromones (Golden and Riddle 1984a; Ilbay and Ambros 2019). Because *P. pacificus* completes the

first J1-J2 molt prior to hatching and emerges as J2 (Lewis and Hong 2014), we hypothesized that the *csu60* incomplete DL belong to a dauer-committed J2 stage, which we designated as J2d. To determine whether the partial DL are pre-DL, or J2 that were unable to complete the morphological transition into full DL, we subjected them to the tests used to define *C. elegans* DL, namely the ability to resist sodium dodecyl sulfate (SDS) (Cassada and Russell 1975) and lack of latex fluorescent bead uptake due to cessation of pharyngeal pumping (Nika et al. 2016).

We found that none of the wild-type, *tu391*, or *csu60* DL ingested fluorescent beads, compared to 84–92% of their J3 counterparts (Figure 8C). A minority of the *csu60* J2d (10%) took up the fluorescent beads, likely due to nominal pharyngeal pumping. The lack of bead uptake in the L2d-dauer lethargus was also observed in *C. elegans* (Nika et al. 2016). Next, we tested whether larvae without beads are also SDS resistant. We found that most of the DL that did not ingest beads survived a subsequent SDS treatment, whereas only 3% of the J2d without beads survived in SDS (Figure 8D, Supplementary Figure S6). This suggests that most J2d needed to undergo the J2-dauer molt that enhanced SDS resistance. Taken together, our results indicate that the prolongation of the pre-dauer J2 stage in *csu60* mutants is morphologically, physiologically, and developmentally equivalent to the L2d in *C. elegans* (Figure 8E).

Discussion

In the wild, *Pristionchus* species associate with beetle hosts as DLs, which resume reproductive development when the hosts die and microbes become available (Herrmann et al. 2007; Meyer et al. 2017). Consequently, the olfactory preferences of *Pristionchus* species have very little overlap with those of *C. elegans*. We show in this study that olfactory profiles are further modulated by a

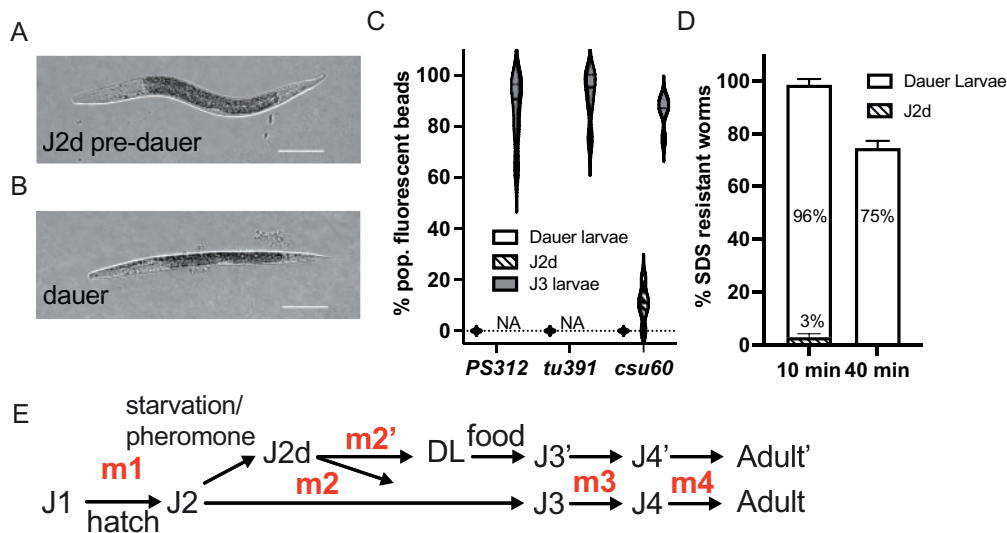


Figure 8 Characterization of *csu60* J2d and DLs. (A, B) A *csu60* J2d pre-dauer lacks a buccal cap and radial constriction, compared to a *csu60* DL. The scale bar is 50 μ m. (C) None of the dauer ($N = 5$, $n_{PS312} = 127$, $n_{tu391} = 137$, $n_{csu60} = 88$) and most of the J3 larvae ($N = 5$, $n_{PS312} = 108$, $n_{tu391} = 82$, $n_{csu60} = 103$) took up fluorescent latex beads after 90 minutes, compared to 10% of *csu60* J2d ($N = 5$, $n = 85$). (D) *csu60* worms that do not take up fluorescent beads are resistant to SDS exposure. Only the *csu60* J2d ($N = 9$, $n = 227$) and DL ($N = 6$, $n = 139$) that lack fluorescent bead uptake were exposed to 1% SDS and monitored for movement after 10 and 40 minutes. J2d ($N = 8$, $n = 38$) and J3 ($N = 6$, $n = 127$) that did ingest fluorescent beads were not resistant to SDS (not shown). Error bars represent s.e.m. (E) Diagram of the *P. pacificus* alternative developmental pathways that share a pre-hatching molt from J1 to J2, followed by 3 post-hatching molts (m). (top) Dauer development occurs under low food conditions, with reversible commitment to dauer entry in the J2d stage, followed by a dauer-specific second molt (m2'), or resumption of reproductive development (m2). Food triggers dauer exit into post-dauer J3 (J3'). (bottom) Reproductive development occurs in the presence of food.

developmental switch that coordinates dauer entry with host odor attraction.

Different steroid hormones mediate dauer formation and host-seeking

In order to effectively compare the olfactory behaviors of adults vs host-seeking DLs, we characterized the first two *Daf-c* loci in the entomophilic nematode *P. pacificus*. We found that deletion of the *Ppa-hsd-2* gene, the sole HSD in *P. pacificus*, results in a *Daf-c* phenotype. This gene is likely responsible for the synthesis of a conserved Δ^7 -DA steroid ligand, which regulates the conserved nuclear hormone receptor DAF-12. Whereas the *Ppa-hsd-2p::cDNA* transgene rescued both the *Ppa-hsd-2(csu60)* *Daf-c* and enhanced host odor attraction phenotypes, exogenous Δ^7 -DA rescued only the *Daf-c* phenotype. One likely possibility is that *Ppa*-HSD-2 produces at least one other type of steroid hormone that acts through a nuclear hormone receptor different from *Ppa*-DAF-12, and this unknown DA/NHR module normally restricts the dauer-specific neuronal development from being executed in the adult stage (Figure 9).

While DAs appear to play a conserved role in promoting reproductive growth across nematode species (Motola et al. 2006; Li et al. 2013; Ma et al. 2019a,c), the specificity of HSDs and their biosynthetic products are likely more divergent and operationally dependent on other dehydrogenases (Mahanti et al. 2014), since their paralogs in each genome can range from none (*Ascaris* and *Toxocaris*) to one (*Pristionchus* and *Brugia*) to three (*Caenorhabditis*) (Patel et al. 2008; Farris et al. 2019). In *C. elegans*, genetic dissection of the relative contribution of the steroidogenic enzymes is confounded by the yet undistinguished roles the HSD-2 and HSD-3 paralogs play in dafachronic acid biosynthesis (Farris et al. 2019). In the vertebrate parasites *Ascaris suum* and *Toxocara canis*, endogenous Δ^4 - and Δ^7 -DA have been detected despite lacking a putative *hsd* ortholog in their genomes, suggesting biosynthesis of DAs can also occur via other enzymes (Ma et al. 2019b). By comparison, the single copy *hsd* in *P. pacificus* may facilitate the structural identification of additional DAs and their

cognate NHRs involved in the proper regulation of developmental stage-specific chemosensation.

The CAN neurons may serve as a source of DA hormones

The lack of conservation in the cell types that express *hsd* homologs between *P. pacificus* and *C. elegans* suggests different cell types could function as sources of DA. In *C. elegans*, *hsd* genes are expressed in the XXX cells (*hsd-1*), the intestine and somatic gonad (*hsd-2*), and the hypodermis (*hsd-3*) (Patel et al. 2008; Farris et al. 2019). The XXX cells also express other components of the steroid hormones important for dauer regulation, including *daf-9* (cytochrome 450) as well as *ncr-1* and *ncr-2* (cholesterol transporters), and are considered neuroendocrine cells in *C. elegans* that act as the source of DA along with the hypodermis (Li et al. 2004; Schaedel et al. 2012). By contrast, *Ppa-hsd-2* expression begins in the J1 stage in the CAN neurons, with expression in the excretory gland cell and the excretory canals during the DL stage. In *C. elegans*, the gland cell is not necessary for molting and dauer entry or exit when ablated during the L1 or L2 stages (Singh and Sulston 1978; Nelson and Riddle 1984), although the gland cell of DLs uniquely lack secretory granules observed in nonstarved developmental stages (Nelson et al. 1983). The *dauerless* gene (*dau-1*) in *P. pacificus* is exclusively expressed in the CAN neurons, and both CAN ablation and *dau-1* mutation increase dauer formation (Mayer et al. 2015). Thus, both inhibitors of dauer formation, *Ppa-hsd-2* and *dau-1*, are expressed in the CAN neurons. It remains to be determined if the *P. pacificus* CANs and excretory cells are endocrine tissues that function to produce and maintain proper DA levels.

Steroid hormones direct neuronal cell fate

The ectopic expression of *Ppa-odr-3p::rfp* in *csu60* and *csu88* shows that *Ppa*-HSD-2 is responsible for maintaining proper cell fate in putative olfactory neurons in *P. pacificus*. However, the addition of 7DA could not rescue this phenotype, suggesting other DAs made by *Ppa*-HSD-2 may be involved in regulating *Ppa-odr-3* expression.

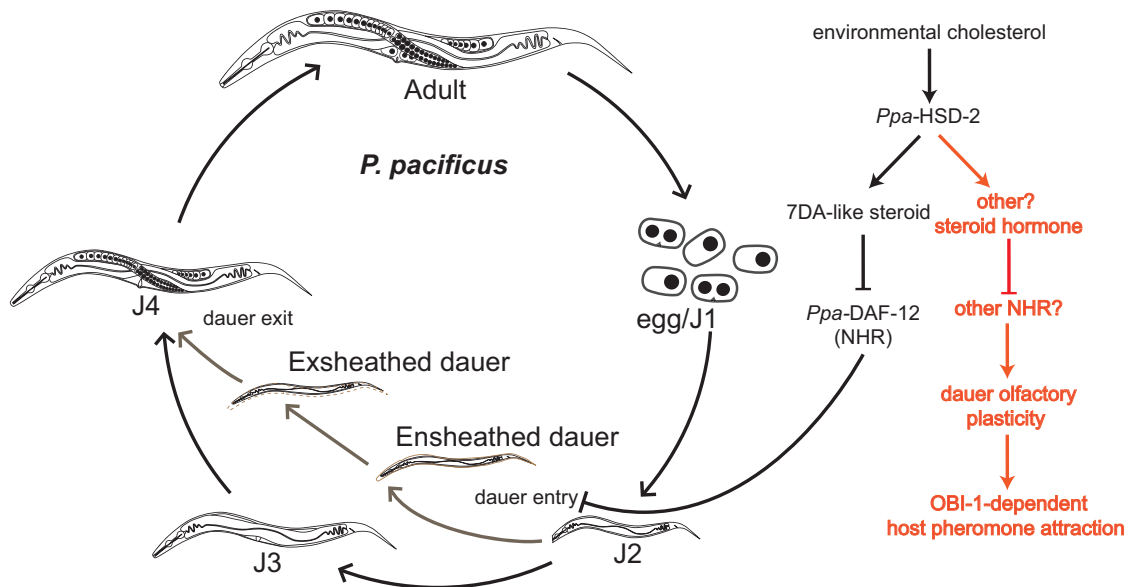


Figure 9 A model for the multiple roles of *Ppa*-HSD-2 in coordinating dauer entry, molting, and olfaction. From the cholesterol precursor, *Ppa*-HSD-2 is required for the synthesis of a Δ^7 -dafachronic acid-like steroid hormone (7DA). Binding of 7DA to the DAF-12 nuclear hormone receptor represses decision for dauer entry. *Ppa*-HSD-2 may also be required for producing other steroid hormones that inhibit the DAF-12-independent and lipid-binding protein OBI-1-dependent dauer-specific host odor attraction in adults.

The homeotic transformation of the AWB to AWC neurons due to mutations in the LIM-4 transcription factor was accompanied by changes in dendritic morphology and chemotaxis behavior (Sagasti et al. 1999). Based on a similar rationale, the loss of *Ppa-hsd-2* could transform AM10(ASI) or AM6(ASG), which are normally involved in inhibiting dauer entry in *C. elegans*, into AM3(AWA) olfactory neurons. Coincidentally, AWA and ASG are sister cells in the *C. elegans* cell lineage (www.wormatlas.org; last accessed May 2021). However, we did not observe fewer *Ppa-che-1p::rfp* expression in the amphid neurons of *Ppa-hsd-2(csue60)* animals (Supplementary Figure S3, C and D), as would be expected if a pair of the neuron mis-expressing *Ppa-odr-3p::rfp* was derived from the AM6(ASG) or AM5(ASE) neurons (Hong et al. 2019). Given the dynamic transcriptional profiles associated with the dauer stage in *P. pacificus* (Sinha et al. 2012), *Daf-c* mutants have the potential to identify genetic circuits coordinating neuronal fate and dauer regulation.

Dauer exsheathment is coupled with dauer entry

Retention of the previous cuticle, or ensheathment, is a hallmark of the infective larvae of many parasitic nematodes as well as insect larvae. In nematodes, the exsheathment of infective larvae in mammalian parasites and EPN often marks the transition to the parasitic phase of the life cycle. Cues for exsheathment are a combination of intrinsic physiological factors, such as the time since emergence from the host, and extrinsic environmental factors, such as temperature or host cues and thus may not be necessarily coupled to dauer entry (Campbell and Gaugler 1991; Wharton 1991; Patel and Wright 1998). For example, exogenous application of an endogenous Δ^7 -DA promotes the exsheathment of iL3 larvae (Ma et al. 2019c). Although there are no candidate genes known to control dauer exsheathment in *C. elegans*—because its dauers do not hold on to their L2 cuticle as long as other species-conserved genes involved in molting may nevertheless modulate the formation of the dauer cuticle. We speculate that the early detachment of the old cuticle in the *Daf-c* DL leads to loss of contact with the mouth plug, resulting in the incarceration of the DL inside the old J2 cuticle. Because dauer entry involves the formation of a buccal cap, the retention of the J2 cuticle in *P. pacificus* DL may render *Daf-c* DL especially prone to the incarcerated phenotype by disrupting the timing or manner of exsheathment.

Although both *Caenorhabditis* and *Pristionchus* species co-occur on rotten vegetation as both DL and feeding stages (Félix et al. 2018), only DL from *Pristionchus* species have been isolated from beetles (Weller et al. 2010; Meyer et al. 2017). The robust chemoattraction to insect-associated pheromones shown by this study supports the model that the DL likely functions as the host-seeking stage of *Pristionchus*. We expect to have a better understanding of how the decision for dauer entry is genetically coordinated with host-associated remodeling of behavior when the cognate olfactory neurons for the host pheromones are identified in *P. pacificus*. Comparisons of the genes regulating dauer development in *C. elegans* and *P. pacificus* could contribute towards a better understanding of how this ancient nematode phenotypic plasticity contributes to the evolution of host associations.

Acknowledgments

The authors thank C. Rödelberger for whole-genome sequence analysis; E. J. Corey for Δ^7 -DA by way of the Sommer lab; J. Ly, J.

Cardenas, and T. Baiocchi for technical assistance; and the Developmental Biology class in Fall 2018 for *csue60* mapping.

Funding

Funding is provided by National Institutes of Health SC3GM105579 (to R.L.H.), NIH 5T34GM008395-29 (to R.V.), NIH R01 441802-HE-31169 (to E.A.H.), and NIH F32AI147617 (to N.B.).

Conflict of interest

None declared.

Literature cited

- Albert PS, Riddle DL. 1983. Developmental alterations in sensory neuroanatomy of the *Caenorhabditis elegans* dauer larva. *J Comp Neurol*. 219:461–481.
- Bargmann CI, Hartwig E, Horvitz HR. 1993. Odorant-selective genes and neurons mediate olfaction in *C. elegans*. *Cell*. 74:515–527.
- Baskaran P, Rödelberger C, Prabh N, Seroby V, Markov GV, et al. 2015. Ancient gene duplications have shaped developmental stage-specific expression in *Pristionchus pacificus*. *BMC Evol Biol*. 15:185.
- Bhattacharya A, Aghayeva U, Berghoff EG, Hobert O. 2019. Plasticity of the electrical connectome of *C. elegans*. *Cell*. 176:1174–1189.e16.
- Bryant AS, Hallem EA. 2018. Terror in the dirt: sensory determinants of host seeking in soil-transmitted mammalian-parasitic nematodes. *Int J Parasitol Drugs Drug Resist*. 8:496–510.
- Butcher RA, Ragains JR, Kim E, Clardy J. 2008. A potent dauer pheromone component in *Caenorhabditis elegans* that acts synergistically with other components. *Proc Natl Acad Sci USA*. 105:14288–14292.
- Campbell LR, Gaugler R. 1991. Effect of exsheathment on motility and pathogenicity of two entomopathogenic nematode species. *J Nematol*. 3:365–370.
- Carrillo MA, Guillermin ML, Rengarajan S, Okubo RP, Hallem EA. 2013. O₂-sensing neurons control CO₂ response in *C. elegans*. *J Neurosci*. 33:9675–9683.
- Cassada RC, Russell RL. 1975. The dauerlarva, a post-embryonic developmental variant of the nematode *Caenorhabditis elegans*. *Dev Biol*. 46:326–342.
- Castelletto ML, Gang SS, Okubo RP, Tselikova AA, Nolan TJ, et al. 2014. Diverse host-seeking behaviors of skin-penetrating nematodes. *PLoS Pathog*. 10:e1004305.
- Cinkornpumin JK, Wisidagama DR, Rapoport V, Go JL, Dieterich C, et al. 2014. A host beetle pheromone regulates development and behavior in the nematode *Pristionchus pacificus*. *Elife*. 3:e03229.
- Dereeper A, Guignon V, Blanc G, Audic S, Buffet S, et al. 2008. Phylogeny.fr: robust phylogenetic analysis for the non-specialist. *Nucleic Acids Res*. 36:W465–W469.
- Dillman AR, Guillermin ML, Lee JH, Kim B, Sternberg PW, et al. 2012. Olfaction shapes host-parasite interactions in parasitic nematodes. *Proc Natl Acad Sci USA*. 109:E2324–E2333.
- Doitsidou M, Poole RJ, Sarin S, Bigelow H, Hobert O. 2010. *C. elegans* mutant identification with a one-step whole-genome-sequencing and SNP mapping strategy. *PLoS One*. 5:e15435.
- Dumas KJ, Guo C, Wang X, Burkhart KB, Adams EJ, et al. 2010. Functional divergence of dafachronic acid pathways in the control of *C. elegans* development and lifespan. *Dev Biol*. 340:605–612.

- Farris M, Fang L, Aslamy A, Pineda V. 2019. Steroid signaling mediates longevity responses to the eat-2 genetic model of dietary restriction in *Caenorhabditis elegans*. *Trans Med Aging*. 3:90–97.
- Félix M-A, Ailion M, Hsu J-C, Richaud A, Wang J. 2018. *Pristionchus nematodes* occur frequently in diverse rotting vegetal substrates and are not exclusively necromenic, while *Panagrellus redivivoides* is found specifically in rotting fruits. *PLoS One*. 13: e0200851.
- Gang SS, Hallem EA. 2016. Mechanisms of host seeking by parasitic nematodes. *Mol Biochem Parasit*. 208:23–32.
- Gems D, Sutton AJ, Sundermeyer ML, Albert PS, King KV, et al. 1998. Two pleiotropic classes of *daf-2* mutation affect larval arrest, adult behavior, reproduction and longevity in *Caenorhabditis elegans*. *Genetics* 150:129–155.
- Golden J, Riddle D. 1982. A pheromone influences larval development in the nematode *Caenorhabditis elegans*. *Science*. 218: 578–580.
- Golden JW, Riddle DL. 1984a. The *Caenorhabditis elegans* dauer larva: developmental effects of pheromone, food, and temperature. *Dev Biol*. 102:368–378.
- Golden JW, Riddle DL. 1984b. A pheromone-induced developmental switch in *Caenorhabditis elegans*: temperature-sensitive mutants reveal a wild-type temperature-dependent process. *Proc Natl Acad Sci USA*. 81:819–823.
- Golden JW, Riddle DL. 1984c. A gene affecting production of the *Caenorhabditis elegans* dauer-inducing pheromone. *Mol Gen Genet*. 3:534–536.
- Hallem EA, Sternberg PW. 2008. Acute carbon dioxide avoidance in *Caenorhabditis elegans*. *Proc Natl Acad Sci USA*. 105:8038–8043.
- Hallem EA, Dillman AR, Hong AV, Zhang Y, Yano JM, et al. 2011. A sensory code for host seeking in parasitic nematodes. *Curr Biol*. 21:377–383.
- Han Z, Lo W-S, Lightfoot JW, Witte H, Sun S, et al. 2020. Improving transgenesis efficiency and CRISPR-associated tools through codon optimization and native intron addition in *Pristionchus nematodes*. *Genetics*. 216:947–956.
- Herrmann M, Mayer WE, Hong RL, Kienle S, Minasaki R, et al. 2007. The nematode *Pristionchus pacificus* (Nematoda: Diplogastriidae) is associated with the oriental beetle *Exomala orientalis* (Coleoptera: Scarabaeidae) in Japan. *Zool Sci*. 24:883–889.
- Hong RL, Sommer RJ. 2006. Chemoattraction in *Pristionchus nematodes* and implications for insect recognition. *Curr Biol*. 16:2359–2365.
- Hong RL, Witte H, Sommer RJ. 2008. Natural variation in *Pristionchus pacificus* insect pheromone attraction involves the protein kinase EGL-4. *Proc Natl Acad Sci USA*. 105:7779–7784.
- Hong RL, Riebesell M, Bumbarger DJ, Cook SJ, Carstensen HR, et al. 2019. Evolution of neuronal anatomy and circuitry in two highly divergent nematode species. *Elife*. 8:e47155.
- Ilbay O, Ambros V. 2019. Pheromones and nutritional signals regulate the developmental reliance on *let-7* family microRNAs in *C. elegans*. *Curr Biol*. 29:1735–1745.e4.
- Jeong P-Y, Jung M, Yim Y-H, Kim H, Park M, et al. 2005. Chemical structure and biological activity of the *Caenorhabditis elegans* dauer-inducing pheromone. *Nature*. 433:541–545.
- Lee JS, Shih P-Y, Schaedel ON, Quintero-Cadena P, Rogers AK, et al. 2017. FMRFamide-like peptides expand the behavioral repertoire of a densely connected nervous system. *Proc Natl Acad Sci USA*. 114:E10726–E10735.
- Lewis VM, Hong RL. 2014. Conserved behavioral and genetic mechanisms in the pre-hatching molt of the nematode *Pristionchus pacificus*. *Evodevo*. 5:31.
- Li J, Brown G, Ailion M, Lee S, Thomas JH. 2004. NCR-1 and NCR-2, the *C. elegans* homologs of the human Niemann-Pick type C1 disease protein, function upstream of DAF-9 in the dauer formation pathways. *Development*. 131:5741–5752.
- Li T-M, Chen J, Li X, Ding X-J, Wu Y, et al. 2013. Absolute quantification of a steroid hormone that regulates development in *Caenorhabditis elegans*. *Anal Chem*. 85:9281–9287.
- Ma G, Wang T, Korhonen PK, Nie S, Reid GE, et al. 2019a. Comparative bioinformatic analysis suggests that specific dauer-like signalling pathway components regulate *Toxocara canis* development and migration in the mammalian host. *Parasite Vector*. 12:32. 10.1186/s13071-018-3265-y
- Ma G, Wang T, Korhonen PK, Stroehlein AJ, Young ND, et al. 2019b. Dauer signalling pathway model for *Haemonchus contortus*. *Parasite Vector*. 12:187. 10.1186/s13071-019-3419-6
- Ma G, Wang T, Korhonen PK, Young ND, Nie S, et al. 2019c. Dafachronic acid promotes larval development in *Haemonchus contortus* by modulating dauer signalling and lipid metabolism. *PLoS Pathog*. 15:e1007960.
- Mahanti P, Bose N, Bethke A, Judkins JC, Wollam J, et al. 2014. Comparative metabolomics reveals endogenous ligands of DAF-12, a nuclear hormone receptor, regulating *C. elegans* development and lifespan. *Cell Metab*. 19:73–83.
- Malone EA, Thomas JH. 1994. A screen for nonconditional dauer-constitutive mutations in *Caenorhabditis elegans*. *Genetics*. 136: 879–886.
- Markov GV, Meyer JM, Panda O, Artyukhin AB, Claaßen M, et al. 2016. Functional conservation and divergence of *daf-22* paralogs in *Pristionchus pacificus* dauer development. *Mol Biol Evol*. 33: 2506–2514.
- Matyash V, Entchev EV, Mende F, Wilsch-Bräuninger M, Thiele C, et al. 2004. Sterol-derived hormone(s) controls entry into diapause in *Caenorhabditis elegans* by consecutive activation of DAF-12 and DAF-16. *PLoS Biol*. 2:e280.
- Mayer MG, Sommer RJ. 2011. Natural variation in *Pristionchus pacificus* dauer formation reveals cross-preference rather than self-preference of nematode dauer pheromones. *Proc Royal Soc B Biol Sci*. 278:2784–2790.
- Mayer MG, Rödelberger C, Witte H, Riebesell M, Sommer RJ. 2015. The orphan gene *dauerless* regulates dauer development and intraspecific competition in nematodes by copy number variation. *PLoS Genet*. 11:e1005146.
- Menti H, Wright DJ, Perry RN. 1997. Desiccation survival of populations of the entomopathogenic nematodes *Steinernema feltiae* and *Heterorhabditis megidis* from Greece and the UK. *J Helminthol*. 71: 41–46.
- Meyer JM, Baskaran P, Quast C, Susoy V, Rödelberger C, et al. 2017. Succession and dynamics of *Pristionchus nematodes* and their microbiome during decomposition of *Oryctes borbonicus* on La Réunion Island. *Environ Microbiol*. 19:1476–1489.
- Moreno E, Lenuzzi M, Rödelberger C, Prabh N, Witte H, et al. 2018. DAF-19/RFX controls ciliogenesis and influences oxygen-induced social behaviors in *Pristionchus pacificus*. *Evol Dev*. 20:233–243.
- Motola DL, Cummins CL, Rottiers V, Sharma KK, Li T, et al. 2006. Identification of ligands for DAF-12 that govern dauer formation and reproduction in *C. elegans*. *Cell*. 124:1209–1223.
- Nakayama K, Ishita Y, Chihara T, Okumura M. 2020. Screening for CRISPR/Cas9-induced mutations using a co-injection marker in the nematode *Pristionchus pacificus*. *Dev Genes Evol*. 230:257–258.
- Nelson FK, Albert PS, Riddle DL. 1983. Fine structure of the *Caenorhabditis elegans* secretory-excretory system. *J Ultrastruct Res*. 82:156–171.
- Nelson FK, Riddle DL. 1984. Functional study of the *Caenorhabditis elegans* secretory-excretory system using laser microsurgery. *J Exp Zool*. 231:45–56.

- Neto MF, Nguyen QH, Marsili J, McFall SM, Voisine C. 2016. The nematode *Caenorhabditis elegans* displays a chemotaxis behavior to tuberculosis-specific odorants. *J Clin Tuberc Other Mycobact Dis.* 4:44–49.
- Nika L, Gibson T, Konkus R, Karp X. 2016. Fluorescent beads are a versatile tool for staging *Caenorhabditis elegans* in different life histories. *G3 (Bethesda).* 6:1923–1933.
- Nuttley WM, Atkinson-Leadbeater KP, van der Kooy D. 2002. Serotonin mediates food-odor associative learning in the nematode *Caenorhabditis elegans*. *Proc Natl Acad Sci USA.* 99:12449–12454.
- Ogawa A, Streit A, Antebi A, Sommer RJ. 2009. A conserved endocrine mechanism controls the formation of dauer and infective larvae in nematodes. *Curr Biol.* 19:67–71.
- Ogawa A, Bento G, Bartelmes G, Dieterich C, Sommer RJ. 2011. *Pristionchus pacificus* *daf-16* is essential for dauer formation but dispensable for mouth form dimorphism. *Development.* 138:1281–1284.
- Ogg S, Paradis S, Gottlieb S, Patterson GI, Lee L. 1997. The Fork head transcription factor DAF-16 transduces insulin-like metabolic and longevity signals in *C. elegans*. *Nature.* 389:994–999.
- O'Halloran DM, Burnell AM. 2003. An investigation of chemotaxis in the insect parasitic nematode *Heterorhabditis bacteriophora*. *Parasitology.* 127:375–385.
- Patel P, Wright D. 1998. The ultrastructure of the cuticle and sheath of infective juveniles of entomopathogenic steinernematid nematodes. *J Helminthol.* 72:257–266.
- Patel DS, Fang LL, Svy DK, Ruvkun G, Li W. 2008. Genetic identification of HSD-1, a conserved steroidogenic enzyme that directs larval development in *Caenorhabditis elegans*. *Development.* 135:2239–2249.
- Penkov S, Ogawa A, Schmidt U, Tate D, Zagoriy V, et al. 2014. A wax ester promotes collective host finding in the nematode *Pristionchus pacificus*. *Nat Chem Biol.* 10:281–285.
- Pradhan S, Quilez S, Homer K, Hendricks M. 2019. Environmental programming of adult foraging behavior in *C. elegans*. *Curr Biol.* 29:2867–2879.e4.
- Rasmann S, Ali JG, Helder J, van der Putten WH. 2012. Ecology and evolution of soil nematode chemotaxis. *J Chem Ecol.* 38:615–628.
- Ren P, Lim C-S, Johnsen R, Albert PS, Pilgrim D, et al. 1996. Control of *C. elegans* larval development by neuronal expression of a TGF- β homolog. *Science* 274:1389–1391.
- Rödelsperger C, Meyer JM, Prabh N, Lanz C, Bemm F, et al. 2017. Single-molecule sequencing reveals the chromosome-scale genomic architecture of the nematode model organism *Pristionchus pacificus*. *Cell Reports.* 21:834–844.
- Ruiz F, Castelletto ML, Gang SS, Hallem EA. 2017. Experience-dependent olfactory behaviors of the parasitic nematode *Heligmosomoides polygyrus*. *PLoS Pathog.* 13:e1006709.
- Sagasti A, Hobert O, Troemel ER, Ruvkun G, Bargmann CI. 1999. Alternative olfactory neuron fates are specified by the LIM homeobox gene *lim-4*. *Gene Dev.* 13:1794–1806.
- Schaedel ON, Gerisch B, Antebi A, Sternberg PW. 2012. Hormonal signal amplification mediates environmental conditions during development and controls an irreversible commitment to adulthood. *PLoS Biol.* 10:e1001306.
- Schroeder FC. 2015. Modular assembly of primary metabolic building blocks: a chemical language in *C. elegans*. *Chem Biol.* 22:7–16.
- Schuster LN, Sommer RJ. 2012. Expressional and functional variation of horizontally acquired cellulases in the nematode *Pristionchus pacificus*. *Gene.* 506:274–282.
- Sieriebriennikov B, Markov GV, Witte H, Sommer RJ. 2017. The role of DAF-21/Hsp90 in mouth-form plasticity in *Pristionchus pacificus*. *Mol Biol Evol.* 34:1644–1653.
- Sims JR, Ow MC, Nishiguchi MA, Kim K, Sengupta P, et al. 2016. Developmental programming modulates olfactory behavior in *C. elegans* via endogenous RNAi pathways. *Elife.* 5:e11642.
- Singh RN, Sulston JE. 1978. Some observations on moulting in *Caenorhabditis elegans*. *Nematol.* 24:63–71.
- Sinha A, Sommer RJ, Dieterich C. 2012. Divergent gene expression in the conserved dauer stage of the nematodes *Pristionchus pacificus* and *Caenorhabditis elegans*. *BMC Genomics.* 13:254.
- Swanson MM, Riddle DL. 1981. Critical periods in the development of the *Caenorhabditis elegans* dauer larva. *Dev Biol.* 84:27–40.
- Turlings TCJ, Hiltbold I, Rasmann S. 2012. The importance of root-produced volatiles as foraging cues for entomopathogenic nematodes. *Plant Soil.* 358:51–60.
- Vidal B, Aghayeva U, Sun H, Wang C, Glenwinkel L, et al. 2018. An atlas of *Caenorhabditis elegans* chemoreceptor expression. *PLoS Biol.* 16:e2004218.
- Weller AM, Mayer WE, Rae R, and Sommer RJ, Weller AM, et al. 2010. Quantitative assessment of the nematode fauna present on geotrupes dung beetles reveals species-rich communities with a heterogeneous distribution. *J Parasitol.* 96:525–531.
- Werner MS, Sieriebriennikov B, Loschko T, Namdeo S, Lenuzzi M, et al. 2017. Environmental influence on *Pristionchus pacificus* mouth form through different culture methods. *Sci Rep.* 7:7207.
- Werner MS, Sieriebriennikov B, Prabh N, Loschko T, Lanz C, et al. 2018. Young genes have distinct gene structure, epigenetic profiles, and transcriptional regulation. *Genome Res.* 28:1675–1687.
- Wharton D. 1991. Ultrastructural changes associated with exsheathment of infective juveniles of *Haemonchus contortus*. *Parasitology.* 103:413–420.
- White JG, Southgate E, Thomson JN, Brenner S. 1986. The structure of the nervous system of the nematode *Caenorhabditis elegans*. *Philos Trans R Soc Lond B Biol Sci.* 314:1–340. 10.1098/rstb.1986.0056
- Witte H, Moreno E, Rödelsperger C, Kim J, Kim J-S, et al. 2015. Gene inactivation using the CRISPR/Cas9 system in the nematode *Pristionchus pacificus*. *Dev Genes Evol.* 225:55–62.
- Zaslav A, Baugh LR, Sternberg PW. 2011. Metazoan operons accelerate recovery from growth-arrested states. *Cell.* 145:981–992.